

QCD phase diagram at high temperature and density

Mei Huang^{1,2} *

¹*Institute of High Energy Physics, Chinese Academy of Sciences, Beijing, China*

²*Theoretical Physics Center for Science Facilities, Chinese Academy of Sciences, Beijing, China*

This article reviews recent progress of QCD phase structure, including color superconductor at high baryon density and strongly interacting quark-gluon plasma (sQGP) at high temperature created through relativistic heavy ion collision. A brief overview is given on the discovery of sQGP at RHIC. The possibility of locating the critical end point (CEP) from the property of bulk viscosity over entropy density is discussed. For the phase structure at high baryon density, the status of the unconventional color superconducting phase with mismatched pairing is reviewed. The chromomagnetic instability, Sarma instability and Higgs instability in the gapless color superconducting phase are clarified.

PACS numbers:

I. INTRODUCTION

Quantum Chromodynamics (QCD) is an asymptotically free theory [1] and regarded as the fundamental theory of quarks and gluons. At very high energies, interaction forces become weak, thus perturbation calculations can be used. The perturbative QCD predictions have been extensively confirmed by experiments, while QCD in the non-perturbative regime is still a challenge to theorists. The fundamental quarks and gluons of QCD have not been seen as free particles, but are always confined within hadrons. It is still difficult to construct the hadrons in terms of nearly massless quarks and gluons. The observed baryon spectrum indicates that the (approximate) chiral symmetry is spontaneously broken in the vacuum. As a result, the eight pseudoscalar mesons π , K and η are light pseudo-Nambu-Goldstone bosons, and the constituent quark obtains dynamical mass, which contributes to the baryon mass. Besides conventional mesons and baryons, QCD itself does not exclude the existence of the non-conventional states such as glueballs, hybrid mesons and multi-quark states [2].

Since 1970s, people have been interested in QCD at extreme conditions. It is expected that the chiral symmetry can be restored, and quarks and gluons will become deconfined at high temperatures and/or densities [3–6]. Fig. 1 is the typical QCD phase diagram, which shows the system is in deconfined quark-gluon plasma phase at high temperature, and in color superconducting phase at high baryon density.

Results from lattice show that the quark-gluon plasma (QGP) does exist. For the system with zero net baryon density, the deconfinement and chiral symmetry restoration phase transitions happen at the same critical temperature [7]. At asymptotically high temperatures, e.g., during the first microseconds of the “Big Bang”, the many-body system composed of quarks and gluons can be regarded as an ideal Fermi and Boson gas. It is believed

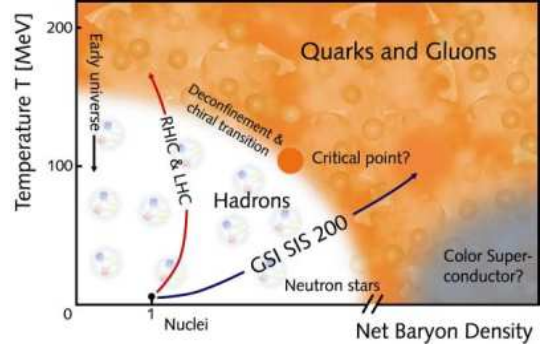


FIG. 1: QCD phase diagram at finite temperature and baryon density.

that the “little Bang” can be produced at RHIC and LHC. Recently, it was shown that the new state of matter produced at RHIC is far away from the asymptotically hot QGP, but in a strongly coupled regime. This state is called strongly coupled quark-gluon plasma (sQGP)[8]. For most recent reviews about QGP, e.g., see Ref. [9–12].

Studying QCD at finite baryon density is the traditional subject of nuclear physics. The behaviour of QCD at finite baryon density and low temperature is central for astrophysics to understand the structure of compact stars, and conditions near the core of collapsing stars (supernovae, hypernovae). Cold nuclear matter, such as in the interior of a Pb nucleus, is at $T = 0$ and $\mu_B \simeq m_N = 940\text{MeV}$. Emerging from this point, there is a first-order nuclear liquid-gas phase transition, which terminates in a critical endpoint at a temperature $\sim 10\text{MeV}$ [13]. If one squeezes matter further and further, nucleons will overlap. Quarks and gluons in one nucleon can feel quarks and gluons in other nucleons. Eventually, deconfinement phase transition will happen. Unfortunately, at the moment, lattice QCD is facing the “sign problem” at nonzero net baryon densities. Our understanding at finite baryon densities has to rely on effective QCD models. Phenomenological models indicated that, at nonzero baryon density, the QGP phase and the hadron gas are separated by a critical line of

*huangm@ihep.ac.cn

roughly a constant energy density $\epsilon_{cr} \simeq 1\text{GeV}/\text{fm}^3$ [14].

In the case of asymptotically high baryon density, the system is a color superconductor. This was proposed by Frautschi [15] and Barrois [16]. Based on the Bardeen, Cooper, and Schrieffer (BCS) theory [17], because there is a weak attractive interaction in the color antitriplet channel, the system is unstable with respect to the formation of particle-particle Cooper-pair condensate in the momentum space. Detailed numerical calculations of color superconducting gaps were firstly carried out by Bailin and Love [18]. They concluded that the one-gluon exchange induces gaps on the order of 1 MeV at several times of nuclear matter density. This small gap has little effect on cold dense quark matter, thus the investigation of cold quark matter lay dormant for several decades. It was only revived recently when it was found that the color superconducting gap can be of the order of 100 MeV [19], which is two orders larger than early perturbative estimates in Ref. [18]. For this reason, the topic of color superconductivity stirred a lot of interest in recent years. For review articles on the color superconductivity, see for example, Refs. [20].

In this article, I will focus on recent progress of sQGP created at RHIC and color superconducting phase structure at intermediate baryon density regime. The outline of this article is as follows: I will give a brief overview on the discovery of sQGP at RHIC in Sec. II. Then introduce the status of the color superconducting phase especially the gapless color superconducting phase in Sec. III. At last, I will give a brief outlook in Sec. IV.

II. STRONGLY INTERACTING QUARK-GLUON PLASMA (SQGP)

A. Discovery of sQGP at RHIC

Studying Quantum chromodynamics (QCD) phase transition and properties of hot quark matter at high temperature has been the main target of heavy ion collision experiments at the Relativistic Heavy Ion collider (RHIC), the forthcoming Large Hadron Collider (LHC) and FAIR at GSI.

The deconfined quark-gluon plasma, if it can be created through heavy-ion collisions, is an intermediate state and cannot be measured directly. In experiment, the detector can only measure the freeze-out hadrons. In order to extract the property of the intermediate state, hydrodynamics is often used to simulate the evolution of the fluid.

The hydrodynamical equations of motion are the local conservation laws of energy-momentum and net charge

$$\partial_\mu T^{\mu\nu} = 0, \quad \partial_\mu N_c^\mu = 0. \quad (1)$$

In ideal hydrodynamics, the energy-momentum tensor takes the form of

$$T_{ideal}^{\mu\nu} = (\epsilon + p)u^\mu u^\nu - pg^{\mu\nu}, \quad (2)$$

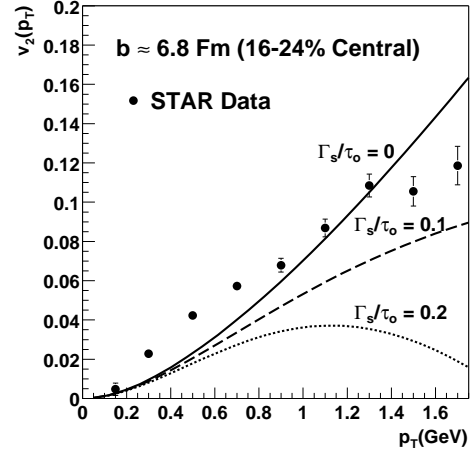


FIG. 2: Elliptic flow v_2 as a function of p_T for different values of Γ_s/τ_0 . The figure taken from Ref.[23].

with u^μ the flow velocity, ϵ, p the energy density and pressure density, respectively.

In the Navier-Stokes hydrodynamics, the energy momentum tensor decomposes into ideal and dissipative parts as

$$T_{NS}^{\mu\nu} = T_{ideal}^{\mu\nu} + \tau^{\mu\nu}, \quad (3)$$

with

$$\tau^{\mu\nu} = \eta(\nabla^\mu u^\nu + \nabla^\nu u^\mu - \frac{2}{3}\Delta^{\mu\nu}\nabla_\alpha u^\alpha + \zeta\Delta^{\mu\nu}\nabla_\alpha u^\alpha). \quad (4)$$

Where $\Delta^{\mu\nu} = g^{\mu\nu} - u^\mu u^\nu$, $\nabla^\mu = \Delta^{\mu\nu}\partial_\nu$, η, ζ are the shear viscosity and bulk viscosity, respectively.

It was expected that deconfined quark matter formed at high temperature should behave like a gas of weakly interacting quark-gluon plasma (wQGP). The perturbative QCD calculation gives a large shear viscosity in the wQGP with $\eta/s \simeq 0.8$ for $\alpha_s = 0.3$ [21]. Therefore, it turned out as a surprise that the RHIC data of elliptic flow v_2 can be described very well by requiring a very small shear viscosity over entropy density ratio η/s [22, 23]. Lattice QCD calculation confirmed that η/s for the purely gluonic plasma is rather small and in the range of 0.1 – 0.2 [24].

It is now believed that the system created at RHIC is a strongly coupled quark-gluon plasma (sQGP) and behaves like a nearly "perfect" fluid [25, 26]. The AdS/CFT duality gives a lower bound $\eta/s = 1/4\pi$ [27]. Therefore, it is conjectured that the sQGP created at RHIC might be the most perfect fluid observed in nature.

However, a perfect fluid should have both vanishing shear and bulk viscosities.

The perturbative QCD calculation gives $\zeta/s = 0.02\alpha_s^2$ for $0.06 < \alpha_s < 0.3$ [28]. In the hydrodynamic simulation used to describe the evolution of the fireball created at RHIC, the bulk viscosity ζ has often been neglected.

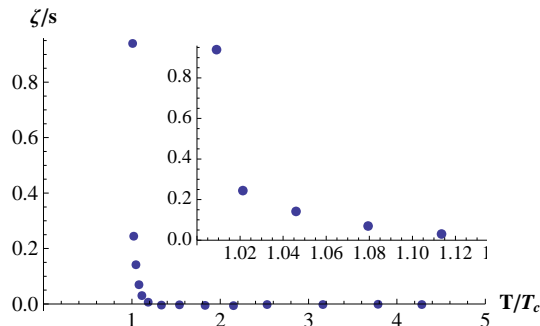


FIG. 3: The bulk viscosity over entropy density ratio as a function of scaled temperature T/T_c . The figure is taken from Ref.[29].

The zero bulk viscosity is for a conformal equation of state and also a reasonable approximation for the weakly interacting gas of quarks and gluons. However, recent lattice QCD results show that the bulk viscosity over entropy density ratio ζ/s rises dramatically up to the order of 1.0 near the critical temperature T_c [29–31]. (There are still some subtle issues to determine the bulk viscosity of QCD through calculating the correlations of the energy-momentum tensor on the lattice, see more detailed discussion in Ref. [32].) The sharp peak of bulk viscosity at T_c has also been observed in the linear sigma model [33] and in the real scalar model [34]. The increasing tendency of ζ/s has been shown in a massless pion gas [35] and in the NJL model below T_c [36]. The large bulk viscosity near phase transition is related to the non-conformal equation of state [37, 38], and the correlation between the bulk viscosity and the conformal anomaly has been investigated in Ref. [39].

The sharp rise of the bulk viscosity will lead to the breakdown of the hydrodynamic approximation around the critical temperature. The effect of large bulk viscosity on hadronization and freeze-out processes of QGP created at heavy ion collisions has been discussed in Refs. [40–43]. The authors of Ref. [40] pointed out the possibility that a sharp rise of bulk viscosity near phase transition induces an instability in the hydrodynamic flow of the plasma, and this mode will blow up and tear the system into droplets. Another scenario is pointed out in Ref. [29, 42] that the large bulk viscosity near phase transition might induce “soft statistical hadronization”, i.e. the expansion of QCD matter close to the phase transition is accompanied by the production of many soft partons, which may be manifested through both a decrease of the average transverse momentum of the resulting particles and an increase in the total particle multiplicity.

B. Searching for the critical end point

At small baryon chemical potential μ , for QCD with two massless quarks, the spontaneously broken chiral symmetry is restored at finite temperature, and it is

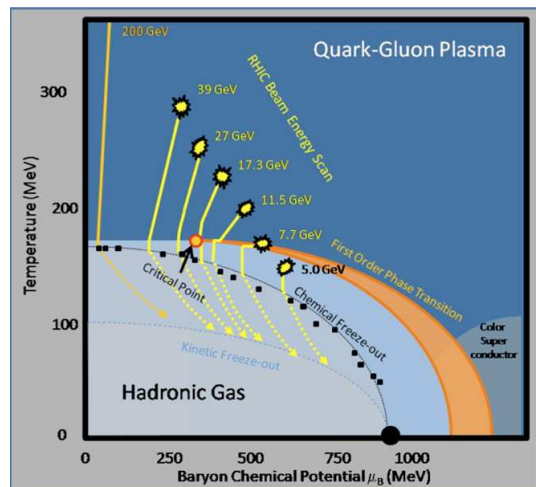


FIG. 4: Searching for the critical end point at RHIC.

shown from lattice QCD [44] and effective QCD models [45] that this phase transition is of second order and belongs to the universality class of $O(4)$ spin model in three dimensions [46]. For real QCD with two quarks of small mass, the second order phase transition becomes a smooth crossover at finite temperature. At finite baryon chemical potential, there are still no reliable results from lattice QCD due to the severe fermion sign problem. However QCD effective models [45] suggest that the chiral phase transition at finite μ is of first order. It is expected that there exists a critical end point (CEP) in the $T - \mu$ QCD phase diagram. The CEP is defined as the end point of the first order phase transition, and belongs to the $Z(2)$ Ising universality class [47]. The signature of CEP has been suggested in Refs. [48]. The precise location of the CEP is still unknown. In the future plan, RHIC is going to lower the energy and trying to locate the CEP as shown in Fig. 4.

Recently, the authors of Ref. [49, 50] suggested using the shear viscosity over entropy density ratio η/s to locate the CEP by observing the ratio of η/s behaves differently in systems of water, helium and nitrogen in first-, second-order phase transitions, see the system of water for example in Fig. 5. The ratio of η/s shows a cusp at T_c for second order phase transition, and a shallow valley near T_c for cross-over, and shows a jump at T_c for first-order phase transition.

Due to the complexity of QCD in the regime of strong coupling, results on hot quark matter from lattice calculation and hydrodynamic simulation are still lack of analytic understanding. In recent years, the anti-de Sitter/conformal field theory (AdS/CFT) correspondence has generated enormous interest in using thermal $\mathcal{N} = 4$ super-Yang-Mills theory (SYM) to understand sQGP. The shear viscosity to entropy density ratio η/s is as small as $1/4\pi$ in the strongly coupled SYM plasma [27]. However, a conspicuous shortcoming of this approach is the conformality of SYM: the square of the speed of sound

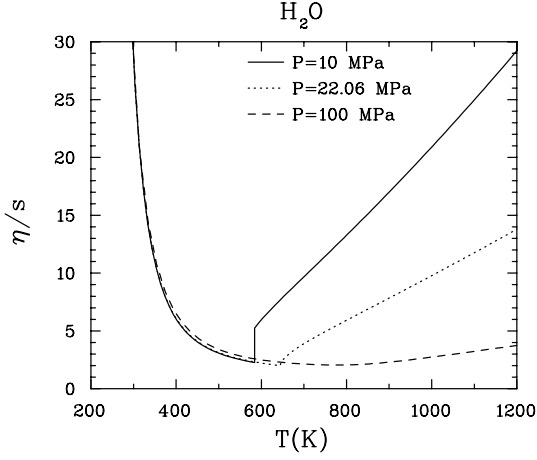


FIG. 5: The shear viscosity over entropy density ratio η/s in the water system. The figure is taken from Ref.[50].

c_s^2 always equals to $1/3$ and the bulk viscosity is always zero at all temperatures in this theory. Though ζ/s at T_c is non-zero for a class of black hole solutions resembling the equation of state of QCD, the magnitude is less than 0.1 [51], which is too small comparing with lattice QCD results.

An alternative nonperturbative approach to study QCD phase transition is by using effective models. In the following, we investigate the thermodynamical and transport properties in two toy models, one is the simplest real scalar model [34, 52], the other is more relativistic QCD effective model, i.e., the Polyakov-linear-sigma model (PLSM) [53], which can describe chiral phase transition as well as deconfinement phase transition successfully.

Real scalar model

We introduce the real scalar theory including the sextet interaction which is described by the Lagrangian

$$\mathcal{L} = \frac{1}{2}(\partial_\mu \phi)^2 - \frac{1}{2}a\phi^2 - \frac{1}{4}b\phi^4 - \frac{1}{6}c\phi^6 + H\phi. \quad (5)$$

When $H = 0$, this theory is invariant under $\phi \rightarrow -\phi$ and has a Z_2 symmetry. here a, b, c are model parameters, which determine the vacuum properties. The system at finite temperature will be evaluated in the Cornwall-Jackiw-Tomboulis (CJT) formalism [54]. We will discuss the following four cases: 1) $c = 0, b > 0, a > 0, H = 0$, the system is always in the symmetric phase. 2) $c = 0, b > 0, a < 0, H = 0$, the vacuum at $T = 0$ breaks the Z_2 symmetry spontaneously, and the symmetry is restored at higher T with a second-order phase transition. 3) $c = 0, b > 0, a < 0, H \neq 0$, the $Z(2)$ symmetry is explicitly broken, and the system will experience a crossover at high temperature. 4) $c > 0, b < 0, a > 0, H = 0$, the broken symmetry is restored at high T with a first-order phase transition.

If symmetry is spontaneously broken in the vacuum, ϕ has a vacuum expectation value $\bar{\phi}$, (in the case of no

symmetry breaking, $\bar{\phi} = 0$ in the vacuum), we shift the field as $\phi \rightarrow \bar{\phi} + \hat{\phi}$. In terms of the shifted field, the Lagrangian is given by

$$\begin{aligned} \mathcal{L} = & \mathcal{L}_0(\bar{\phi}) + \frac{1}{2}(\partial_\mu \hat{\phi})^2 - \frac{1}{2}m_0^2\hat{\phi}^2 - (b\bar{\phi} + \frac{10}{3}c\bar{\phi}^3)\hat{\phi}^3 \\ & - (\frac{b}{4} + \frac{5}{2}c\bar{\phi}^2)\hat{\phi}^4 - c\bar{\phi}\hat{\phi}^5 - \frac{1}{6}c\hat{\phi}^6, \end{aligned} \quad (6)$$

with

$$\mathcal{L}_0(\bar{\phi}) = \frac{a}{2}\bar{\phi}^2 + \frac{b}{4}\bar{\phi}^4 + \frac{c}{6}\bar{\phi}^6 - H\bar{\phi}. \quad (7)$$

It is noticed that the new field $\hat{\phi}$ obtains a tree-level mass of $m_0^2 = a + 3b\bar{\phi}^2 + 5c\bar{\phi}^4$. The induced interaction terms including the cubic interaction term with coupling strength $b\bar{\phi} + 10/3c\bar{\phi}^3$, the quartic term with coupling strength $b/4 + 5/2c\bar{\phi}^2$, the quintic term with coupling strength $c\bar{\phi}$, and the six-point interaction term with coupling strength $1/6c$.

Assuming translation invariance, we consider effective potential Ω instead of effective action Γ , these two quantities are related via:

$$\Gamma = -\frac{V}{T}\Omega, \quad (8)$$

where V is the 3-volume of the system. The effective potential in the CJT formalism reads

$$\begin{aligned} \Omega[\bar{\phi}, \bar{G}] = & \Omega_0(\bar{\phi}) + \Omega_2[\bar{\phi}, \bar{G}] \\ & + \frac{1}{2} \int_K [\ln \bar{G}^{-1}(K) + \bar{G}_0^{-1}(K) \bar{G}(K) - 1] \end{aligned} \quad (9)$$

where $\Omega_0(\bar{\phi}) = \mathcal{L}_0(\bar{\phi})$ is the tree-level potential, and $\bar{G}(\bar{G}_0)$ is the full(tree-level) propagator:

$$\bar{G}^{-1}(K, \bar{\phi}) = -K^2 + M^2(\bar{\phi}), \quad \bar{G}_0^{-1}(K, \bar{\phi}) = -K^2 + m_0^2(\bar{\phi}). \quad (10)$$

In the Hartree approximation, the momentum dependent contributions are neglected, Ω_2 denotes the contribution from two-particle irreducible diagrams, and takes the form of

$$\Omega_2[\bar{\phi}, \bar{G}] = \left(\frac{3}{4}b + \frac{15}{2}c\bar{\phi}^2 \right) \left(\int_K \bar{G}(K) \right)^2 + \frac{15}{6}c \left(\int_K \bar{G}(K) \right)^3. \quad (11)$$

The self-consistent one- and two-point Green's functions satisfy

$$\frac{\delta \Omega}{\delta \bar{\phi}} \Big|_{\bar{\phi}=\phi, \bar{G}=G} \equiv 0, \quad \frac{\delta \Omega}{\delta \bar{G}} \Big|_{\bar{\phi}=\phi, \bar{G}=G} \equiv 0. \quad (12)$$

All thermodynamical information of the system is contained in the grand canonical potential Ω , evaluated at the mean field level. The entropy density s is determined by taking the derivative of effective potential with respect to the temperature, i.e.,

$$s = -\partial \Omega(\phi) / \partial T. \quad (13)$$

As the standard treatment in lattice calculation, we introduce the normalized pressure density p which is normalized to vanish at $T = \mu = 0$ and the energy density ε as

$$p = -\Omega, \quad \varepsilon = -p + Ts. \quad (14)$$

The equation of state $p(\varepsilon)$ is an important input into hydrodynamics. The square of the speed of sound C_s^2 is related to p/ε and has the form of

$$C_s^2 = \frac{dp}{d\varepsilon} = \frac{s}{Tds/dT} = \frac{s}{C_v}, \quad (15)$$

where

$$C_v = \partial\varepsilon/\partial T, \quad (16)$$

is the specific heat. At the critical temperature, the entropy density as well as the energy density change most quickly with temperature, thus one expect that C_s^2 should have a minimum at T_c .

The shear viscosity η is calculated by using the Boltzmann equation [55]. The two-particle elastic scattering amplitude, which governs particle collisions in the Boltzmann equation, is

$$i\mathcal{T} = \lambda_4 + \lambda_3^2 \left[\frac{1}{s-m^2} + \frac{1}{t-m^2} + \frac{1}{u-m^2} \right], \quad (17)$$

where s, t and u are Mandelstam variables, and $\lambda_3 = 6\phi_0(b + \frac{10c}{3}\phi_0^2 + 10c \int_K \tilde{G}(K, \tilde{\phi}))$ and $\lambda_4 = 12(\frac{b}{2} + 5c\phi_0^2 + 5c \int_K \tilde{G}(K, \tilde{\phi}))$ are effective couplings.

The shear viscosity over entropy density ratio η/s in the real scalar model is shown in Fig.6 and 7 for different orders of phase transitions. There is clearly a qualitative difference in the η/s behavior between cases with and without a phase transition. It is seen that η/s shows a cusp at T_c for the case of 2nd-order phase transition, a shallow valley near T_c for crossover, and shows a jump at T_c for the case of 1st-order phase transition. This behavior is qualitatively the same as that in the classic systems such as the in H_2O system as shown in Fig. 5. If there is no phase transition, η/s is always monotonically decreasing.

The bulk viscosity is related to the correlation function of the trace of the energy-momentum tensor θ_μ^μ :

$$\zeta = \frac{1}{9} \lim_{\omega \rightarrow 0} \frac{1}{\omega} \int_0^\infty dt \int d^3r e^{i\omega t} \langle [\theta_\mu^\mu(x), \theta_\mu^\mu(0)] \rangle. \quad (18)$$

According to the result derived from low energy theorem, in the low frequency region, the bulk viscosity takes the form of [29, 30]

$$\begin{aligned} \zeta &= \frac{1}{9\omega_0} \left\{ T^5 \frac{\partial}{\partial T} \left(\frac{\varepsilon - 3p}{T^4} \right) + 16|\varepsilon_v| \right\}, \\ &= \frac{1}{9\omega_0} \{ -16\varepsilon + 9TS + TC_v + 16|\varepsilon_v| \}. \end{aligned} \quad (19)$$

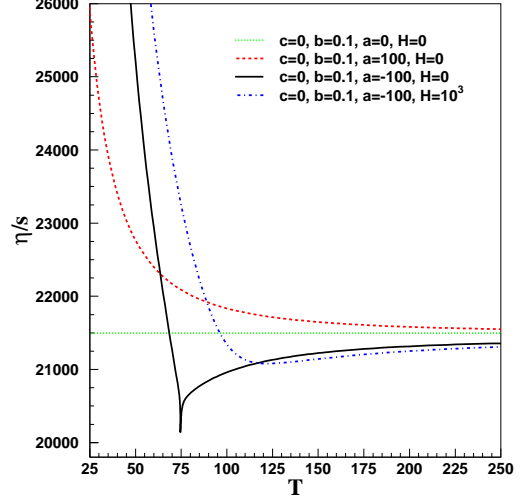


FIG. 6: The shear viscosity over entropy density η/s as a function of the temperature T , for cases with a second-order phase transition (solid curve), a crossover (dash-dotted curve), and with no phase transition for massive field (dashed curve) and massless field (dotted curve). The figure is taken from Ref.[52].

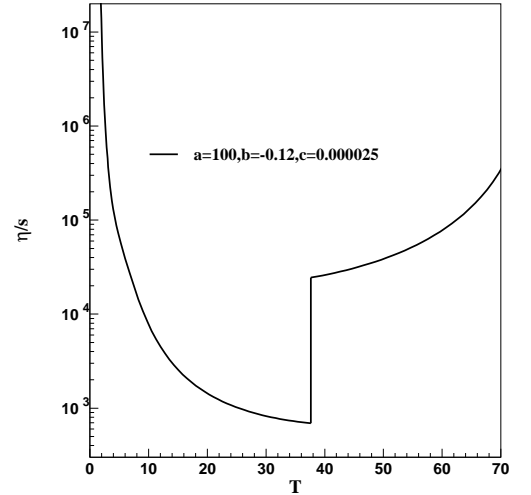


FIG. 7: The shear viscosity over entropy density η/s as a function of the temperature T , for the case of 1st order phase transition.

with the negative vacuum energy density $\varepsilon_v = \Omega_v = \Omega(\phi)|_{T=0}$, and the parameter $\omega_0 = \omega_0(T)$ is a scale at which the perturbation theory becomes valid. From the above formula, we can see that the bulk viscosity is proportional to the specific heat C_v near phase transition, thus ζ/s behaves as $1/C_s^2$ near T_c in this approximation.

The bulk viscosity over entropy density ratio ζ/s as a function of T is shown in Figs.8,9,10, and 11. It is shown

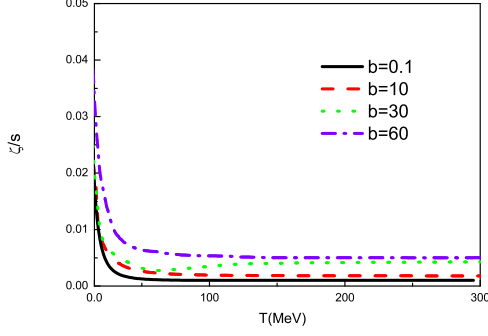


FIG. 8: The bulk viscosity over entropy density ζ/s as a function of T for the case without phase transition in the real scalar model. The figure is taken from Ref.[34].

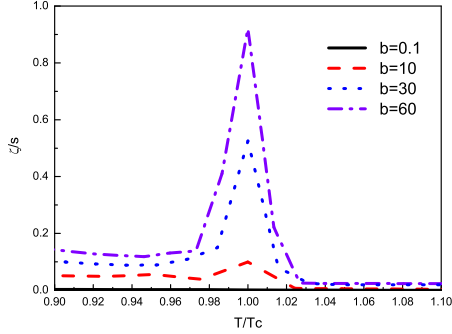


FIG. 9: The bulk viscosity over entropy density ζ/s as a function of T for a 2nd-order phase transition in the real scalar model in the real scalar model. The figure is taken from Ref.[34].

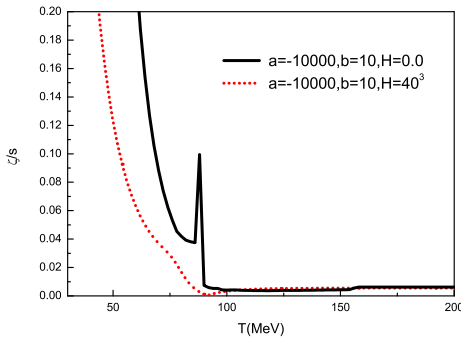


FIG. 10: The bulk viscosity over entropy density ζ/s as a function of T for the case of crossover (the solid line). The figure is taken from Ref.[34].

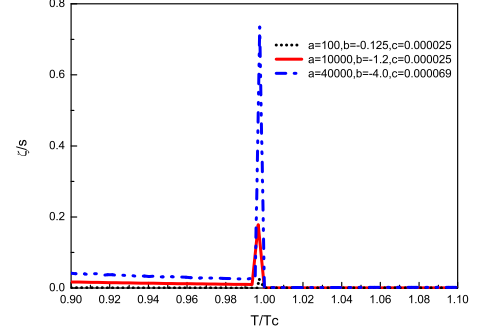


FIG. 11: The bulk viscosity over entropy density ζ/s as a function of T for a 1st-order phase transition in the real scalar model. The figure is taken from Ref.[34].

that in the case without symmetry breaking, the bulk viscosity over entropy density ζ/s decreases monotonically with the increase of the temperature. In the case of 2nd-order phase transition, ζ/s decreases with T at low temperature region, then rises up at the critical temperature T_c and shows an upward cusp, and decreases further in the temperature $T > T_c$. In the case of crossover, it is observed the cusp behavior of ζ/s is washed out. In the case of 1st-order phase transition, ζ/s shows divergent behavior at T_c .

From Refs.[50, 52], we know that η/s shows a shallow valley in the case of crossover and a jump at T_c for first-order phase transition. But it is hard to distinguish whether the system experiences a crossover or first-order phase transition just from the value of η/s extracted from the elliptic flow v_2 .

From our results in the real scalar model, it is found that the ratio of ζ/s shows a very sharp peak at T_c in the case of first order phase transition, and there is no obvious change of ζ/s for crossover. As pointed out in Ref. [40] that a sharp rise of bulk viscosity near phase transition induces an instability in the hydrodynamic flow of the plasma, and this mode will blow up and tear the system into droplets. Therefore, one can distinguish whether the system experiences a first order phase transition or a crossover from observables at RHIC experiments. This result supports the idea of using ζ/s to locate the CEP as suggested in Ref. [30].

The Polyakov-linear-sigma model

We have shown the behavior of shear viscosity over entropy density η/s and bulk viscosity over entropy density ζ/s near T_c for different orders of phase transitions in a toy model, i.e, the real scalar model. In the following, we use a more realistic QCD effective model, i.e, the Polyakov-linear-sigma model (PLSM), which is described by the Lagrangian [56]

$$\mathcal{L} = \mathcal{L}_{chiral} - \mathcal{U}(\phi, \phi^*, T) \quad (20)$$

where we have separated the contribution of chiral degrees of freedom and the Polyakov loop. The chiral part of the Lagrangian, $\mathcal{L}_{chiral} = \mathcal{L}_q + \mathcal{L}_m$ consists of the fermionic part

$$\mathcal{L}_q = \sum_f \bar{\psi}_f (i\gamma^\mu D_\mu - gT_a(\sigma_a + i\gamma_5\pi_a))\psi_f \quad (21)$$

and the purely mesonic contribution

$$\begin{aligned} \mathcal{L}_m = & \text{Tr}(\partial_\mu \Phi^\dagger \partial^\mu \Phi - m^2 \Phi^\dagger \Phi) - \lambda_1 [\text{Tr}(\Phi^\dagger \Phi)]^2 \\ & - \lambda_2 \text{Tr}(\Phi^\dagger \Phi)^2 + c[\text{Det}(\Phi) + \text{Det}(\Phi^\dagger)] \\ & + \text{Tr}[H(\Phi + \Phi^\dagger)], \end{aligned} \quad (22)$$

the sum is over the three flavors (f=1,2,3 for u, d, s). In the above equation we have introduced a flavor-blind Yukawa coupling g of the quarks to the mesons and the coupling of the quarks to a background gauge field $A_\mu = \delta_{\mu 0} A_0$ via the covariant derivative $D_\mu = \partial_\mu - iA_\mu$. The Φ is a complex 3×3 matrix and is defined in terms of the scalar σ_a and pseudoscalar π_a meson nonets,

$$\Phi = T_a(\sigma_a + i\pi_a). \quad (23)$$

The 3×3 matrix H breaks the symmetry explicitly and is chosen as

$$H = T_a h_a, \quad (24)$$

where h_a are nine external fields. The $T_a = \lambda_a/2$ are the generators of the $U(3)$ symmetry, λ_a are the Gell-Mann matrices with $\lambda_0 = \sqrt{\frac{2}{3}}\mathbf{1}$. The T_a are normalized to $\text{Tr}(T_a T_b) = \delta_{ab}/2$ and obey the $U(3)$ algebra with $[T_a, T_b] = if_{abc}T_c$ and $\{T_a, T_b\} = d_{abc}T_c$ respectively, here f_{abc} and d_{abc} for $a, b, c = 1, \dots, 8$ are the standard antisymmetric and symmetric structure constants of $SU(3)$ group and

$$f_{ab0} \equiv 0, \quad d_{ab0} = \sqrt{\frac{2}{3}}\delta_{ab}. \quad (25)$$

The quantity $\mathcal{U}(\phi, \phi^*, T)$ is the Polyakov-loop effective potential expressed by the dynamics of the traced Polyakov loop

$$\phi = (\text{Tr}_c L)/N_c, \quad \phi^* = (\text{Tr}_c L^\dagger)/N_c. \quad (26)$$

The Polyakov loop L is a matrix in color space and explicitly given by

$$L(\vec{x}) = \mathcal{P} \exp \left[i \int_0^\beta d\tau A_4(\vec{x}, \tau) \right], \quad (27)$$

with $\beta = 1/T$ being the inverse of temperature and $A_4 = iA^0$. In the Polyakov gauge, the Polyakov-loop matrix can be given as a diagonal representation [57]. The coupling between Polyakov loop and quarks is uniquely determined by the covariant derivative D_μ in the PLSM

Lagrangian in Eq.(20), and in the chiral limit, this Lagrangian is invariant under the chiral flavor group, just like the original QCD Lagrangian. The trace of the Polyakov-loop, ϕ and its conjugate ϕ^* can be treated as classical field variables in this work.

The temperature dependent effective potential $\mathcal{U}(\phi, \phi^*, T)$ is used to reproduce the thermodynamical behavior of the Polyakov loop for the pure gauge case in accordance with lattice QCD data, and it has the $Z(3)$ center symmetry like the pure gauge QCD Lagrangian. In the absence of quarks, we have $\phi = \phi^*$ and the Polyakov loop is taken as an order parameter for deconfinement. For low temperatures, \mathcal{U} has a single minimum at $\phi = 0$, while at high temperatures it develops a second one which turns into the absolute minimum above a critical temperature T_0 , and the $Z(3)$ center symmetry is spontaneously broken. In this paper, we will use the potential $\mathcal{U}(\phi, \phi^*, T)$ proposed in Ref.[58], which has a polynomial expansion in ϕ and ϕ^* :

$$\frac{\mathcal{U}(\phi, \phi^*, T)}{T^4} = -\frac{b_2(T)}{2}|\phi|^2 - \frac{b_3}{6}(\phi^3 + \phi^{*3}) + \frac{b_4}{4}(|\phi|^2)^2, \quad (28)$$

with

$$b_2(T) = a_0 + a_1 \left(\frac{T_0}{T}\right) + a_2 \left(\frac{T_0}{T}\right)^2 + a_3 \left(\frac{T_0}{T}\right)^3. \quad (29)$$

A precision fit of the constants a_i, b_i is performed to reproduce the lattice data for pure gauge theory thermodynamics and the behavior of the Polyakov loop as a function of temperature. The corresponding parameters are

$$\begin{aligned} a_0 = 6.75, \quad a_1 = -1.95, \quad a_2 = 2.625, \\ a_3 = -7.44, \quad b_3 = 0.75, \quad b_4 = 7.5. \end{aligned} \quad (30)$$

The critical temperature T_0 for deconfinement in the pure gauge sector is fixed at 270 MeV, in agreement with the lattice results.

we obtain the thermodynamical potential density as

$$\Omega(T, \mu_f) = \frac{-T \ln \mathcal{Z}}{V} = U(\sigma_x, \sigma_y) + \mathcal{U}(\phi, \phi^*, T) + \Omega_{\bar{\psi}\psi}, \quad (31)$$

with the quarks and antiquarks contribution

$$\begin{aligned} \Omega_{\bar{\psi}\psi} = & -2TN_q \int \frac{d^3\vec{p}}{(2\pi)^3} \{ \\ & \ln[1 + 3(\phi + \phi^* e^{-(E_q - \mu)/T})e^{-(E_q - \mu)/T} + e^{-3(E_q - \mu)/T}] \\ & + \ln[1 + 3(\phi^* + \phi e^{-(E_q + \mu)/T})e^{-(E_q + \mu)/T} + e^{-3(E_q + \mu)/T}] \} \\ & -2TN_s \int \frac{d^3\vec{p}}{(2\pi)^3} \{ \\ & \ln[1 + 3(\phi + \phi^* e^{-(E_s - \mu)/T})e^{-(E_s - \mu)/T} + e^{-3(E_s - \mu)/T}] \\ & + \ln[1 + 3(\phi^* + \phi e^{-(E_s + \mu)/T})e^{-(E_s + \mu)/T} + e^{-3(E_s + \mu)/T}] \}. \end{aligned} \quad (32)$$

Here, $N_q = 2$, $N_s = 1$, and $E_q = \sqrt{\vec{p}^2 + m_q^2}$ is the valence quark and antiquark energy for u and d quarks, for strange quark s , it is $E_s = \sqrt{\vec{p}^2 + m_s^2}$, and m_q , m_s is the constituent quark mass for u , d and s . The purely mesonic potential is

$$U(\sigma_x, \sigma_y) = \frac{m^2}{2}(\sigma_x^2 + \sigma_y^2) - h_x \sigma_x - h_y \sigma_y - \frac{c}{2\sqrt{2}} \sigma_x^2 \sigma_y^2 + \frac{\lambda_1}{2} \sigma_x^2 \sigma_y^2 + \frac{1}{8}(2\lambda_1 + \lambda_2) \sigma_x^4 + \frac{1}{4}(\lambda_1 + \lambda_2) \sigma_y^4. \quad (33)$$

Minimizing the thermodynamical potential in Eq.(31) with respect to σ_x , σ_y , ϕ and ϕ^* , we obtain a set of equations of motion

$$\frac{\partial \Omega}{\partial \sigma_x} = 0, \quad \frac{\partial \Omega}{\partial \sigma_y} = 0, \quad \frac{\partial \Omega}{\partial \phi} = 0, \quad \frac{\partial \Omega}{\partial \phi^*} = 0. \quad (34)$$

The set of equations can be solved for the fields as functions of temperature T and chemical potential μ , and the solutions of these coupled equations determine the behavior of the chiral order parameter σ_x , σ_y and the Polyakov loop expectation values ϕ , ϕ^* as a function of T and μ .

Fig.12 shows the pressure density over energy density p/ε , which is represented in terms of equation-of-state (EOS) parameter, at zero density and finite density, respectively. We observe that the pressure density over energy density increases with temperature and saturates at high temperature. Both the linear sigma model and the Polyakov linear sigma model give very similar results at high temperature, the pressure density over energy density p/ε saturates at a value smaller than $1/3$. Another common feature of the p/ε in the linear sigma model and the Polyakov linear sigma model is that there is a bump appearing at low temperature region, which is also observed in the lattice result. Around the critical temperature T_c , the pressure density over energy density p/ε shows a downward cusp. However, the minimum value of the p/ε around T_c is 0.2 in the linear sigma model, which is much larger than the result from the Polyakov linear sigma model and the lattice QCD data. For the Polyakov linear sigma model, the minimum of p/ε around T_c is 0.075, which is consistent with the lattice QCD data [38].

In Fig.13, we plot the bulk viscosity over entropy density ratio ζ/s as a function of the temperature for zero chemical potential. It is shown that, at zero chemical potential $\mu = 0$, the bulk viscosity over entropy density ζ/s decreases monotonically with the increase of the temperature in both the Polyakov linear sigma model and linear sigma model, and at high temperature, ζ/s reaches its conformal value 0. In [30], the bulk viscosity over entropy density of the three flavor system is extracted from lattice result, which is shown by the square. It is observed that ζ/s in PLSM near phase transition is in very good agreement with the lattice result in [30], i.e., it rises sharply near phase transition.

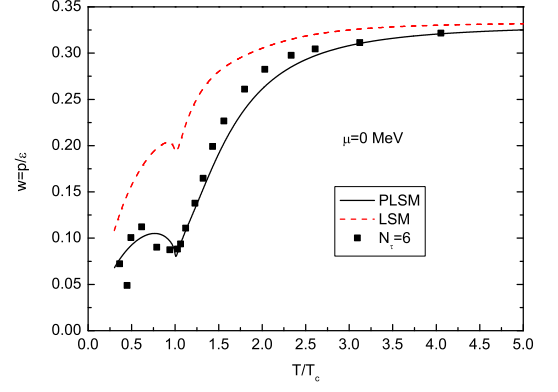


FIG. 12: The equation-of-state parameter $w(T) = p(T)/\varepsilon(T)$ for $\mu = 0$ MeV. The Polyakov linear sigma model prediction (solid line) and the linear sigma model prediction (dash line) are compared with $N_f = 2 + 1$ lattice QCD data for $N_\tau = 6$. Lattice data taken from Ref.[38]. The figure is taken from Ref.[53].

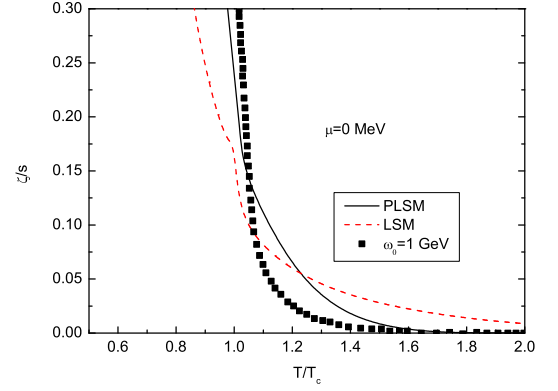


FIG. 13: The bulk viscosity over entropy density ratio ζ/s as a function of the temperature for $\mu = 0$ MeV. The solid line denotes the Polyakov linear sigma model prediction and the dashed line denotes the linear sigma model prediction. Lattice data taken from Ref.[30]. The figure is taken from Ref.[53].

In Ref. [34], we have investigated the equation of state and bulk viscosity in the real scalar model and $O(4)$ model in the case of 2nd order phase transition, crossover and 1st order phase transition, and we have found that the thermodynamic properties and transport properties in these simple models near the critical temperature T_c at strong coupling are similar to those of the complex QCD system. In a more realistic QCD effective model, i.e., the Polyakov linear sigma model [53], we have systematically investigated the thermodynamic properties and bulk viscosity and found these properties match with lattice data very well in the case of zero chemical potential. We further evaluate the chiral phase transitions of u , d and s quarks and deconfinement phase transition at finite temperature and finite density, and show the $T - \mu$ phase structure of the Polyakov linear sigma model in Fig.14.

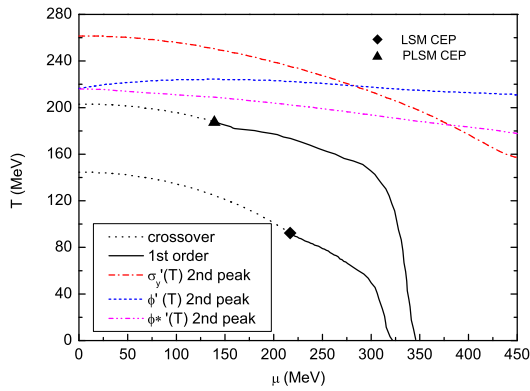


FIG. 14: The $T - \mu$ phase diagram in the Polyakov linear sigma model. The figure is taken from Ref.[53].

For the Polyakov linear sigma model, the result shows that the critical end point is around $(T_E, \mu_E) = (188 \text{ MeV}, 139.5 \text{ MeV})$, which is close to the lattice result $(T_E, \mu_E) = (162 \pm 2 \text{ MeV}, \mu_E = 120 \pm 13 \text{ MeV})$ [59]. For the linear sigma model without the Polyakov loop, the critical end point is located at $(T_E, \mu_E) \simeq (92.5 \text{ MeV}, 216 \text{ MeV})$. The critical chemical potential μ_E in PLSM is much lower than that in the PNJL model with three quark flavors where the predicted critical end point is $\mu_E > 300 \text{ MeV}$ [60, 61].

The chiral phase transition for the strange quark and the deconfinement phase transition in the $T - \mu$ plane are shown by the dash-dotted line and dotted line, respectively. It is found that with the increase of chemical potential, the critical temperature for strange quark to restore chiral symmetry decreases. However, for the deconfinement phase transition, with the increase of chemical potential, the deconfinement critical temperature keeps almost a constant around 220 MeV. It can be seen that in the Polyakov linear sigma model, there exists two-flavor quarkyonic phase [62] at low density, where the u, d quarks restore chiral symmetry but still in confinement, and three-flavor quarkyonic phase at high density, where the u, d, s quarks restore chiral symmetry but still in confinement.

Because the Polyakov-loop in the PLSM is not introduced dynamically, it is difficult to calculate the transport properties from the Boltzmann equation. However, we can use Eq.(19) to calculate the bulk viscosity. In Fig.15, we plot the bulk viscosity over entropy density ratio ζ/s as a function of the temperature for different chemical potentials. It shows ζ/s as function of the scaled temperature T/T_c for different chemical potentials with $\mu = 0, 80, 139.5, 160 \text{ MeV}$. We can see that when the chemical potential increases up to $\mu = 80 \text{ MeV}$, there is an upward cusp appearing in ζ/s right at the critical temperature T_c . With the increase of the chemical potential, the upward cusp becomes sharper, and the height of the cusp increases. At the critical end point μ_E and when $\mu > \mu_E$ for the first order phase transition, ζ/s becomes

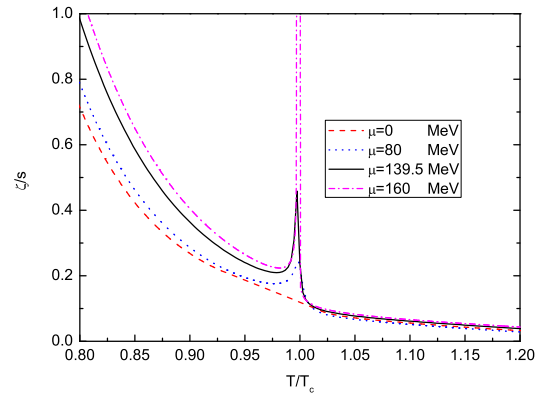


FIG. 15: The bulk viscosity over entropy density ratio ζ/s in the PLSM for different chemical potentials as functions of T/T_c . The figure is taken from Ref.[53].

divergent at the critical temperature.

As discussed earlier, the sharp rise of the bulk viscosity will lead to the breakdown of the hydrodynamic approximation around the critical temperature, and will affect the hadronization and freeze-out processes of QGP created at heavy ion collisions Refs. [40–43]. For example, in Ref. [40], it is pointed out that a sharp rise of bulk viscosity near phase transition might induce an instability in the hydrodynamic flow of the plasma, and this mode will blow up and tear the system into droplets. Another scenario is pointed out in Ref. [29, 42] that the large bulk viscosity near phase transition might induce “soft statistical hadronization”, i.e. the expansion of QCD matter close to the phase transition is accompanied by the production of many soft partons, which may be manifested through both a decrease of the average transverse momentum of the resulting particles and an increase in the total particle multiplicity. Therefore the critical end point might be located through the observables which are sensitive to the ratio of bulk viscosity over entropy density.

However, it is noticed that the results of bulk viscosity in this paper are based on Eq. (19), where the ansatz for the spectral function

$$\frac{\rho(\omega, \vec{0})}{\omega} = \frac{9\zeta}{\pi} \frac{\omega_0^2}{\pi(\omega^2 + \omega_0^2)} \quad (35)$$

has been used in the small frequency, and ω_0 is a scale at which the perturbation theory becomes valid. In our calculation, $\omega_0 = 1 \text{ GeV}$, its magnitude at T_c is in agreement with that obtained in ChPT for massive pion gas system in Ref. [39]. Qualitatively, the bulk viscosity corresponds to nonconformality, thus it is reasonable to observe a sharp rising of bulk viscosity near phase transition. Ref. [39] has investigated the correlation between the bulk viscosity and conformal breaking, and supports the results in Ref.[29, 30]. The sharp rising of bulk viscosity has also been observed by another lattice result [31] and in the linear sigma model [33]. However, till

now, no full calculation has been done for the bulk viscosity. The frequency dependence of the spectral density has been analyzed in Refs. [63] and [32] and the limitation of the ansatz Eq.(35) has been discussed. From Eq. (19), we see that the bulk viscosity is dominated by C_v at T_c . If C_v diverges at T_c , the bulk viscosity should also be divergent at the critical point and behave as $t^{-\alpha}$. However, the detailed analysis in the Ising model in Ref. [64] shows a very different divergent behavior $\zeta \sim t^{-z\nu+\alpha}$, with $z \simeq 3$ the dynamic critical exponent and $\nu \simeq 0.630$ the critical exponent in the Ising system. More careful calculation on the bulk viscosity is needed in the future.

III. COLOR SUPERCONDUCTING PHASES

It is known that the deconfined cold dense quark matter is in color superconducting phase.

Let us start with the system of free fermion gas. Fermions obey the Pauli exclusion principle, which means no two identical fermions can occupy the same quantum state. The energy distribution for fermions (with mass m) has the form of

$$f(E_p) = \frac{1}{e^{\beta(E_p - \mu)} + 1}, \quad \beta = 1/T, \quad (36)$$

here $E_p = \sqrt{p^2 + m^2}$, μ is the chemical potential and T is the temperature. At zero temperature, $f(E_p) = \theta(\mu - E_p)$. The ground state of the free fermion gas is a filled Fermi sea, i.e., all states with the momenta less than the Fermi momentum $p_F = \sqrt{\mu^2 - m^2}$ are occupied, and the states with the momenta greater than the Fermi momentum p_F are empty. Adding or removing a single fermion costs no free energy at the Fermi surface.

For the degenerate Fermi gas, the only relevant fermion degrees of freedom are those near the Fermi surface. Considering two fermions near the Fermi surface, if there is a net attraction between them, it turns out that they can form a bound state, i.e., Cooper pair [65]. The binding energy of the Cooper pair $\Delta(K)$ (K the total momentum of the pair), is very sensitive to K , being a maximum where $K = 0$. There is an infinite degeneracy among pairs of fermions with equal and opposite momenta at the Fermi surface. Because Cooper pairs are composite bosons, they will occupy the same lowest energy quantum state at zero temperature and produce a Bose-Einstein condensation. Thus the ground state of the Fermi system with a weak attractive interaction is a complicated coherent state of particle-particle Cooper pairs near the Fermi surface [17]. Exciting a quasiparticle and a hole which interact with the condensate requires at least the energy of 2Δ .

In QED case in condensed matter, the interaction between two electrons by exchanging a photon is repulsive. The attractive interaction to form electron-electron Cooper pairs is by exchanging a phonon, which is a collective excitation of the positive ion background. The

Cooper pairing of the electrons breaks the electromagnetic gauge symmetry, and the photon obtains an effective mass. This indicates the Meissner effect [66], i.e., a superconductor expels the magnetic fields.

In QCD case at asymptotically high baryon density, the dominant interaction between two quarks is due to the one-gluon exchange. This naturally provides an attractive interaction between two quarks. The scattering amplitude for single-gluon exchange in an $SU(N_c)$ gauge theory is proportional to

$$(T_a)_{ki}(T_a)_{lj} = -\frac{N_c + 1}{4N_c}(\delta_{jk}\delta_{il} - \delta_{ik}\delta_{jl}) \quad (37) \\ + \frac{N_c - 1}{4N_c}(\delta_{jk}\delta_{il} + \delta_{ik}\delta_{jl}).$$

Where T_a is the generator of the gauge group, and i, j and k, l are the fundamental colors of the two quarks in the incoming and outgoing channels, respectively. Under the exchange of the color indices of either the incoming or the outgoing quarks, the first term is antisymmetric, while the second term is symmetric. For $N_c = 3$, Eq. (38) represents that the tensor product of two fundamental colors decomposes into an (antisymmetric) color antitriplet and a (symmetric) color sextet,

$$[\mathbf{3}]^c \otimes [\mathbf{3}]^c = [\bar{\mathbf{3}}]_a^c \oplus [\mathbf{6}]_s^c. \quad (38)$$

In Eq. (38), the minus sign in front of the antisymmetric contribution indicates that the interaction in this antitriplet channel is attractive, while the interaction in the symmetric sextet channel is repulsive.

For cold dense quark matter, the attractive interaction in the color antitriplet channel induces the condensate of the quark-quark Cooper pairs, and the ground state is called the “color superconductivity”. Since the diquark cannot be color singlet, the diquark condensate breaks the local color $SU(3)_c$ symmetry, and the gauge bosons connected with the broken generators obtain masses. Comparing with the Higgs mechanism of dynamical gauge symmetry breaking in the Standard Model, here the diquark Cooper pair can be regarded as a composite Higgs particle. The calculation of the energy gap and the critical temperature from the first principles has been derived systematically in Refs. [67–74].

In reality, we are more interested in cold dense quark matter at moderate baryon density regime, i.e., $\mu_q \sim 500 \text{ MeV}$, which may exist in the interior of neutron stars. It is likely that cold dense quark droplet might be created in the laboratory through heavy ion collisions in GSI-SPS energy scale. At these densities, an extrapolation of the asymptotic arguments becomes unreliable, we have to rely on effective models. Calculations in the framework of pointlike four-fermion interactions based on the instanton vertex [19, 75–77], as well as in the Nambu–Jona-Lasinio (NJL) model [78–82] show that color superconductivity does occur at moderate densities, and the magnitude of diquark gap is around 100 MeV.

A. Different color superconducting phases

Even though the antisymmetry in the attractive channel signifies that only quarks with different colors can form Cooper pairs, color superconductivity has very rich phase structure because of its flavor, spin and other degrees of freedom. In the following, I list some of the known color superconducting phases.

The 2SC phase

Firstly we consider a system with only massless u and d quarks, assuming that the strange quark is much heavier than the up and down quarks. The color superconducting phase with only two flavors is normally called the 2SC phase.

Renormalization group arguments [67, 83, 84] suggest that possible quark pairs always condense in the s -wave. This means that the spin wave function of the pair is anti-symmetric. Since the diquark condenses in the color antitriplet $\bar{\mathbf{3}}_c$ channel, the color wave function of the pair is also anti-symmetric. The Pauli principle requires that the total wave function of the Cooper pair has to be anti-symmetric under the exchange of the two quarks forming the pair. Thus the flavor wave function has to be anti-symmetric, too. This determines the structure of the order parameter

$$\Delta_{ij}^{\alpha\beta} = \Delta \epsilon_{ij} \epsilon^{\alpha\beta b}, \quad (39)$$

where color indices $\alpha, \beta \in (r, g, b)$ and flavor indices $i, j \in (u, d)$. From the order parameter Eq. (39), we can see that the condensate picks a color direction (here the *blue* direction, which is arbitrarily selected). The ground state is invariant under an $SU(2)_c$ subgroup of the color rotations that mixes the red and green colors, but the blue quarks are singled out as different. Thus the color $SU(3)_c$ is broken down to its subgroup $SU(2)_c$, and five of the gluons obtain masses, which indicates the Meissner effect [85].

In the 2SC phase, the Cooper pairs are $ud - du$ singlets and the global flavor symmetry $SU(2)_L \otimes SU(2)_R$ is intact, i.e., the chiral symmetry is not broken. There is also an unbroken global symmetry which plays the role of $U(1)_B$. Thus no global symmetry are broken in the 2SC phase.

The CFL phase

In the case when the chemical potential is much larger than the strange quark mass, we can assume $m_u = m_d = m_s = 0$, and there are three degenerate massless flavors in the system. The spin-0 order parameter should be color and flavor anti-symmetric, which has the form of

$$\Delta_{ij}^{\alpha\beta} = \Delta \sum_I \epsilon_{ijI} \epsilon^{\alpha\beta I}, \quad (40)$$

where color indices $\alpha, \beta \in (r, g, b)$ and flavor indices $i, j \in (u, d, s)$. Writing $\sum_I \epsilon_{ijI} \epsilon^{\alpha\beta I} = \delta_i^\alpha \delta_j^\beta - \delta_j^\alpha \delta_i^\beta$, we can see

that the order parameter

$$\Delta_{ij}^{\alpha\beta} = \Delta (\delta_i^\alpha \delta_j^\beta - \delta_j^\alpha \delta_i^\beta) \quad (41)$$

describes the color-flavor locked (CFL) phase proposed in Ref. [86]. Many other different treatments [87–89] agreed that a condensate of the form (40) is the dominant condensate in three-flavor QCD.

In the CFL phase, all quark colors and flavors participate in the pairing. The color gauge group is completely broken, and all eight gluons become massive [86, 90], which ensures that there are no infrared divergences associated with gluon propagators. Electromagnetism is no longer a separate symmetry, but corresponds to gauging one of the flavor generators. A rotated electromagnetism (“ \tilde{Q} ”) remains unbroken.

Two global symmetries, the chiral symmetry and the baryon number, are broken in the CFL phase, too. In zero-density QCD, the spontaneous breaking of chiral symmetry is due to the condensation of left-handed quarks with right-handed quarks. Here, at high baryon density, the chiral symmetry breaking occurs due to a rather different mechanism: locking of the flavor rotations to color. In the CFL phase, there is only pairing of left-handed quarks with left-handed quarks, and right-handed quarks with right-handed quarks, i.e.,

$$\langle \psi_{Li}^\alpha \psi_{Lj}^\beta \rangle = - \langle \psi_{Ri}^\alpha \psi_{Rj}^\beta \rangle. \quad (42)$$

Where L, R indicate left- and right-handed, respectively, α, β are color indices and i, j are flavor indices. A gauge invariant form [91, 92]

$$\begin{aligned} \langle \psi_{Li}^\alpha \psi_{Lj}^\beta \bar{\psi}_{R\alpha}^k \bar{\psi}_{R\beta}^l \rangle &\sim \langle \psi_{Li}^\alpha \psi_{Lj}^\beta \rangle \langle \bar{\psi}_{R\alpha}^k \bar{\psi}_{R\beta}^l \rangle \\ &\sim \Delta^2 \epsilon_{ijm} \epsilon^{klm} \end{aligned} \quad (43)$$

captures the chiral symmetry breaking. The spectrum of excitations in the CFL phase contains an octet of Goldstone bosons associated with the chiral symmetry breaking. This looks remarkably like those at low density. In the excitation spectrum of the CFL phase, there is another singlet $U(1)$ Goldstone boson related to the baryon number symmetry breaking, which can be described using the order parameter

$$\langle udsuds \rangle \sim \langle \Lambda \Lambda \rangle. \quad (44)$$

In QCD with three degenerate light flavors, the spectrum in the CFL phase looks similar to that in the hypernuclear phase at low-density. It is suggested that the low density hyper-nuclear phase and the high density quark phase might be continuously connected [93].

Spin-1 color superconductivity

In the case of only one-flavor quark system, due to the antisymmetry in the color space, the Pauli principle requires that the Cooper pair has to occur in a symmetric spin channel. Therefore, in the simplest case, the Cooper

pairs carry total spin one. Spin-1 color superconductivity was firstly studied in Ref. [18], for more recent and detailed discussions about the spin-1 gap, its critical temperature and Meissner effect, see Refs. [69, 70, 94–97]. For a review, see Ref. [98].

Pairing with mismatch: LOFF, CFL-K, g2SC and gCFL

To form the Cooper pair, the ideal case is when the two pairing quarks have the same Fermi momenta, i.e., $p_{F,i} = p_{F,j}$ with $p_{F,i} = \sqrt{\mu_{F,i}^2 - m_i^2}$, like in the ideal 2SC, CFL, and spin-1 color superconducting phases. However, in reality, the nonzero strange quark mass or the requirement of charge neutrality induces a mismatch between the Fermi momenta of the two pairing quarks. When the mismatch is very small, it has little effect on the Cooper pairing. While if the mismatch is very large, the Cooper pair will be destroyed. The most interesting situation happens when the mismatch is neither very small nor very large.

LOFF: In the regime just on the edge of decoupling of the two pairing quarks (due to the nonzero strange quark mass for the qs Cooper pair with $q \in (u, d)$ or the chemical potential difference for the ud Cooper pair), a “LOFF” (Larkin-Ovchinnikov-Fulde-Ferrell) state may be formed. The LOFF state was firstly investigated in the context of electron superconductivity in the presence of magnetic impurities [99, 100]. It was found that near the unpairing transition, it is favorable to form a state in which the Cooper pairs have nonzero momentum. This is favored because it gives rise to a regime of phase space where each of the two quarks in a pair can be close to its Fermi surface, and such pairs can be created at low cost in free energy. This sort of condensates spontaneously break translational and rotational invariance, leading to gaps which vary periodically in a crystalline pattern. The crystalline color superconductivity has been investigated in a series of papers, e.g., see Refs. [101–108].

CFL-K: The strange quark mass m_s induces an effective chemical potential $\mu_s = m_s^2/(2p_F)$, and the effects of the strange quark mass can be quite dramatic. In the CFL phase, the K^+ and K^0 modes may be unstable for large values of the strange quark mass to form a kaon condensation [109–112]. In the framework of effective theory [91, 92, 113–115], the masses of the Goldstone bosons can be determined as

$$\begin{aligned} m_{\pi^\pm} &= \mp \frac{m_d^2 - m_u^2}{2p_F} + \left[\frac{4A}{f_\pi^2} (m_u + m_d)m_s \right]^{1/2}, \\ m_{K^\pm} &= \mp \frac{m_s^2 - m_u^2}{2p_F} + \left[\frac{4A}{f_\pi^2} (m_u + m_s)m_d \right]^{1/2}, \\ m_{K^0, \bar{K}^0} &= \mp \frac{m_s^2 - m_d^2}{2p_F} + \left[\frac{4A}{f_\pi^2} (m_s + m_d)m_u \right]^{1/2}, \end{aligned} \quad (45)$$

with $A = 3\Delta^2/(4\pi^2)$ [92, 116]. It was found that the kaon

masses are substantially affected by the strange quark mass, the masses of K^- and \bar{K}^0 are pushed up while K^+ and K^0 are lowered. As a result, the K^+ and K^0 become massless if $m_s|_{crit} = 3.03 m_d^{1/3} \Delta^{2/3}$. For larger values of m_s the kaon modes are unstable, signaling the formation of a kaon condensate. Recently, it was found that in the CFL phase, there also may exist η condensate [117].

g2SC and gCFL: When the β -equilibrium and the charge neutrality condition are required for the two-flavor quark system, the Fermi surfaces of the pairing u quark and d quark differ by μ_e , here μ_e is the chemical potential for electrons. It was found that when the gap parameter $\Delta < \mu_e/2$, the system will be in a new ground state called the gapless 2SC (g2SC) phase [118]. The g2SC phase has very unusual temperature properties [119] and chromomagnetic properties [120]. This phase will be introduced in more detail in Sec. IIIB.

Similarly, for a charge neutral 3-flavor system with a nonzero strange quark mass m_s , with increasing m_s , the CFL phase transfers to a new gapless CFL (gCFL) phase when $m_s^2/\mu \simeq 2\Delta$ [121]. The finite temperature property of the charge neutral three-flavor quark matter was investigated in Ref. [122–124]. Recently, it was shown that the kaon condensate shifts the critical strange quark mass to higher values for the appearance of the gCFL phase [125].

B. Gapless color superconductor

In this section, I would like to focus on unconventional color superconductor with mismatched pairing by taking charge neutral two-flavor system as an example.

It is very likely that the color superconducting phase may exist in the core of compact stars, where bulk matter should satisfy the charge neutrality condition. This is because bulk matter inside the neutron star is bound by the gravitation force, which is much weaker than the electromagnetic and the strong color forces. Any electric charges or color charges will forbid the formation of bulk matter. In addition, matter inside neutron star also needs to satisfy the β -equilibrium.

In the ideal two-flavor color superconducting (2SC) phase, the pairing u and d quarks have the same Fermi momenta. Because u quark carries electric charge $2/3$, and d quark carries electric charge $-1/3$, it is easy to check that quark matter in the ideal 2SC phase is positively charged. To satisfy the electric charge neutrality condition, roughly speaking, twice as many d quarks as u quarks are needed. This induces a large difference between the Fermi surfaces of the two pairing quarks, i.e., $\mu_d - \mu_u = \mu_e \approx \mu/4$, where μ, μ_e are chemical potentials for quarks and electrons, respectively. Naively, one would expect that the requirement of the charge neutrality condition will destroy the ud Cooper pairing in the 2SC phase.

Indeed, the interest in the charge neutral 2SC phase was stirred by the paper Ref. [126]. It was claimed in this

paper that there will be no 2SC phase inside neutron star under the requirement of the charge neutrality condition. In fact, the authors meant that for a charge neutral three flavor system, the 2SC+s phase is not favorable compared to the CFL phase. This is a natural result under the assumption of a *small* strange quark mass, even without the requirement of the charge neutrality condition. In the framework of the bag model, in which the strange quark mass is very small, the CFL phase is always the ground state for cold dense quark matter, and there is no space for the existence of two-flavor quark matter.

However, there is another scenario about the hadron-quark phase transition in the framework of the SU(3) NJL model. In the vacuum, quarks obtain their dynamical masses induced by the chiral condensate. u, d quarks have constituent mass around 330 MeV, while the s quark has heavier constituent mass, which is around 500 MeV. With the increasing of the baryon density, the constituent quark mass starts to decrease when the chemical potential becomes larger than its vacuum constituent mass. In this scenario, s quark restores chiral symmetry at a larger critical chemical potential than that of u, d quarks. If the deconfinement phase transition happens sequentially, there will exist some baryon density regime for only u, d quark matter and s quark is still too heavy to appear in the system.

It is worth to mention that the effect of the electric charge neutrality condition on a three-flavor quark system is very different from that on a two-flavor quark system. Because s quark carries $-1/3$ electric charges, it is much easier to neutralize the electric charges in a three-flavor quark system than that in a two-flavor quark system. However, the color charge neutrality condition is nontrivial in a three-flavor quark system, when the strange quark mass is not very small. For a detailed consideration of the charge neutral three-flavor system, see recent papers Refs. [121–124].

In the following, we focus on the charge neutral two flavor quark system. Motivated by the sequential deconfinement scenario, the authors of Ref. [127] investigated charge neutral quark matter based on the SU(3) NJL model. To large extent, their results agree with those in Ref. [126], i.e., the CFL phase is more favorable than the 2SC+s phase in charge neutral three-flavor cold dense quark matter, and they did not find the charge neutral 2SC phase.

However, it was found in Ref. [128] that a charge neutral two-flavor color superconducting (N2SC) phase does exist, which was confirmed in Refs. [129, 130]. Comparing with the ideal 2SC phase, the N2SC phase found in Ref. [128] has a largely reduced diquark gap parameter, and the pairing quarks have different number densities. The latter contradicts the pairing ansatz in Ref. [131]. Therefore, one could suggest that this phase is an unstable Sarma state [132]. In Ref. [118], it was shown that the N2SC phase is a stable state under the restriction of the charge neutrality condition. As a by-product, which comes out as a very important feature, it was

found that the quasi-particle spectrum has zero-energy excitation in this charge neutral two-flavor color superconducting phase. Thus this phase is named the “gapless 2SC(g2SC)” phase.

The 2-flavor system can be described by the gauged Nambu–Jona-Lasinio (gNJL) model, the Lagrangian density has the form of

$$\mathcal{L} = \bar{q}(i\not{D} + \hat{m}\gamma^0)q + G_S[(\bar{q}q)^2 + (\bar{q}i\gamma^5\vec{\tau}q)^2] + G_D[\bar{q}^C i\gamma^5\tau_2\epsilon^{\rho}q][\bar{q}i\gamma^5\tau_2\epsilon^{\rho}q^C], \quad (46)$$

with $D_\mu \equiv \partial_\mu - igA_\mu^a T^a$. Here A_μ^a are gluon fields, $T^a = \lambda^a/2$ are the generators of $SU(3)_c$ gauge group with $a = 1, \dots, 8$. In the gNJL model, the gauge fields are external fields and do not contribute to the dynamics of the system. The property of the color superconducting phase characterized by the diquark gap parameter is determined by the nonperturbative gluon fields, which has been simply replaced by the four-fermion interaction in the NJL model. G_S and G_D are the quark-antiquark coupling constant and the diquark coupling constant, respectively. $q^C = C\bar{q}^T$, $\bar{q}^C = q^T C$ are charge-conjugate spinors, $C = i\gamma^2\gamma^0$ is the charge conjugation matrix (the superscript T denotes the transposition operation). The quark field $q \equiv q_{i\alpha}$ with $i = u, d$ and $\alpha = r, g, b$ is a flavor doublet and color triplet, as well as a four-component Dirac spinor, $\tau = (\tau^1, \tau^2, \tau^3)$ are Pauli matrices in the flavor space, where τ^2 is antisymmetric, and $(\epsilon)^{ik} \equiv \epsilon^{ik}$, $(\epsilon^b)^{\alpha\beta} \equiv \epsilon^{\alpha\beta b}$ are totally antisymmetric tensors in the flavor and color spaces.

In β -equilibrium, the matrix of chemical potentials in the color-flavor space $\hat{\mu}$ is given in terms of the quark chemical potential μ , the chemical potential for the electrical charge μ_e and the color chemical potential μ_8 ,

$$\mu_{ij}^{\alpha\beta} = (\mu\delta_{ij} - \mu_e Q_{ij})\delta^{\alpha\beta} + \frac{2}{\sqrt{3}}\mu_8\delta_{ij}(T_8)^{\alpha\beta}. \quad (47)$$

The total thermodynamic potential for u, d quarks in β -equilibrium with electrons takes the form [118, 119, 128]:

$$\Omega_{u,d,e} = -\frac{1}{12\pi^2} \left(\mu_e^4 + 2\pi^2 T^2 \mu_e^2 + \frac{7\pi^4}{15} T^4 \right) + \frac{m^2}{4G_S} + \frac{\Delta^2}{4G_D} - \sum_A \int \frac{d^3p}{(2\pi)^3} \left[E_A + 2T \ln \left(1 + e^{-E_A/T} \right) \right] \quad (48)$$

where the electron mass was taken to be zero, which is sufficient for the purposes of the current study. The sum over A runs over all (6 quark and 6 antiquark) quasi-particles. The explicit dispersion relations and the degeneracy factors of the quasi-particles read

$$E_{ub}^\pm = E(p) \pm \mu_{ub}, \quad [\times 1] \quad (49)$$

$$E_{db}^\pm = E(p) \pm \mu_{db}, \quad [\times 1] \quad (50)$$

$$E_{\Delta^\pm}^\pm = E_\Delta^\pm(p) \pm \delta\mu. \quad [\times 2] \quad (51)$$

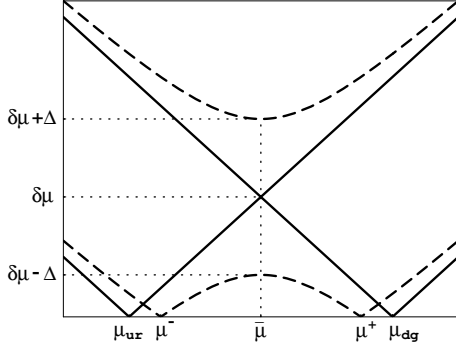


FIG. 16: Dispersion relation of the gapless phase. The figure is taken from Ref. [118].

Gapless excitation in quasi-particle spectrum

It is instructive to start with the excitation spectrum in the case of the ideal 2SC phase when $\delta\mu = 0$. With the conventional choice of the gap pointing in the anti-blue direction in the color space, the blue quarks are not affected by the pairing dynamics, and the other four quasi-particle excitations are linear superpositions of $u_{r,g}$ and $d_{r,g}$ quarks and holes. The quasi-particle is nearly identical with a quark at large momenta and with a hole at small momenta. We represent the quasi-particle in the form of $Q(\text{quark}, \text{hole})$, then the four quasi-particles can be represented explicitly as $Q(u_r, d_g)$, $Q(u_g, d_r)$, $Q(d_r, u_g)$ and $Q(d_g, u_r)$. When $\delta\mu = 0$, the four quasi-particles are degenerate, and have a common gap Δ . If there is a small mismatch ($\delta\mu < \Delta$) between the Fermi surfaces of the pairing u and d quarks, the excitation spectrum will change. It is found that $\delta\mu$ induces two different dispersion relations, the quasi-particle $Q(d_g, u_r)$ has a smaller energy gap $\Delta - \delta\mu$, and the quasi-particle $Q(u_r, d_g)$ has a larger energy gap $\Delta + \delta\mu$. This is similar to the case when the mismatch is induced by the mass difference of the pairing quarks [133].

If the mismatch $\delta\mu$ is larger than the gap parameter Δ , the lower dispersion relation for the quasi-particle $Q(d_g, u_r)$ will cross the zero-energy axis, as shown in the right panel of Fig. 16. The energy of the quasi-particle $Q(d_g, u_r)$ vanishes at two values of momenta $p = \mu^-$ and $p = \mu^+$ where $\mu^\pm \equiv \bar{\mu} \pm \sqrt{(\delta\mu)^2 - \Delta^2}$. Thus this phase is called the gapless 2SC (g2SC) phase.

Thermal stable charge neutral g2SC state

An unstable gapless CFL phase has been found in Ref. [133], and a similar stable gapless color superconductivity could also appear in a cold atomic gas [134] or in u, s or d, s quark matter when the number densities are kept fixed [135]. Also, some gapless phases may appear due to P-wave interactions in the cold atomic system [136]. However, the gapless 2SC phase is a thermal stable state under the charge neutrality condition.

If a macroscopic chunk of quark matter exists inside compact stars, it must be neutral with respect to electric

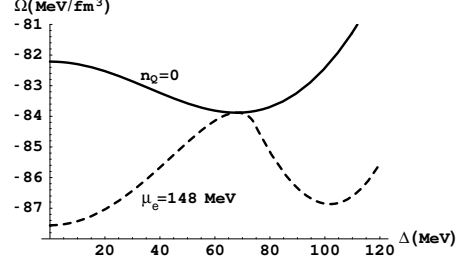


FIG. 17: The effective potential as a function of the diquark gap Δ calculated at a fixed value of the electric chemical potential $\mu_e = 148$ MeV (dashed line), and the effective potential defined along the neutrality line (solid line). The results are plotted for $\mu = 400$ MeV with $\eta = 0.75$. The figure is taken from Ref. [118].

as well as color charges. Now, we discuss the role of the electric charge neutrality condition. If a macroscopic chunk of quark matter has nonzero net electric charge density n_Q , the total thermodynamic potential for the system should be given by

$$\Omega = \Omega_{Coulomb} + \Omega_{u,d,e}, \quad (52)$$

where $\Omega_{Coulomb} \sim n_Q^2 V^{2/3}$ (V is the volume of the system) is induced by the repulsive Coulomb interaction. The energy density grows with increasing the volume of the system, as a result, it is almost impossible for matter inside stars to remain charged over macroscopic distances. So bulk quark matter must satisfy electric neutrality condition with $\Omega_{Coulomb}|_{n_Q=0} = 0$, and $\Omega_{u,d,e}|_{n_Q=0}$ is on the neutrality line. Under the charge neutrality condition, the total thermodynamic potential of the system is $\Omega|_{n_Q=0} = \Omega_{u,d,e}|_{n_Q=0}$.

Here, we want to emphasize that: The proper way to find the ground state of homogeneous neutral u, d quark matter is to minimize the thermodynamic potential along the neutrality line $\Omega|_{n_Q=0} = \Omega_{u,d,e}|_{n_Q=0}$. This is different from that in the flavor asymmetric quark system, where β -equilibrium is required but μ_e is a free parameter, and the ground state for flavor asymmetric quark matter is determined by minimizing the thermodynamic potential $\Omega_{u,d,e}$. At a fixed $\mu_e = 148$ MeV and with color charge neutrality, the thermodynamic potential is shown as a function of the diquark gap by the dashed line in Fig. 17. The minimum gives the ground state of the flavor asymmetric system, and the corresponding diquark gap is $\Delta = 0$, but this state has negative electric charge density, and cannot exist in the interior of compact stars.

C. Chromomagnetic instability in the g2SC phase

As we know, one of the most important properties of the ordinary superconductor is its Meissner effect,

i.e., a superconductor expels the magnetic field, which was discovered by Meissner and Ochsenfeld in 1933 [66]. From the theoretical point of view, the Meissner effect can be explained using the linear response theory. The induced current j_i^{ind} is related to the magnetic field A_j by $j_i^{ind} = \Pi_{ij} A_j$, where the response function Π_{ij} is the photon polarization tensor. The response function has two components, diamagnetic and paramagnetic part [137]. In the static and long-wavelength limit, for the normal metal, the paramagnetic component cancels exactly the diamagnetic component. While in the superconducting phase, the paramagnetic component is quenched by the energy gap and producing a net diamagnetic response. Thus the ordinary superconductor is a perfect diamagnet.

In color superconducting phases, the gluon self-energy (the response function to an external color field), has been investigated in the ideal 2SC phase [85] and in the CFL phase [90]. The results show that the gauge bosons connected with the broken generators obtain masses in these phases, which indicate the Meissner screening effect in these phases.

It is very interesting to know the chromomagnetic property in the g2SC phase. We studied the g2SC phase in the framework of the SU(2) NJL model, and the NJL model lacks gluons. As reflection of this, it possesses the global instead of gauged color symmetry. In addition, there appear five Nambu-Goldstone (NG) bosons in the ground state of the model when the color symmetry is broken. In QCD, there is no room for such NG bosons. However, the NJL model can be thought of as the low energy theory of QCD in which the gluons, as independent degrees of freedom, are integrated out. The gluons could be reintroduced back by gauging the color symmetry in the Lagrangian density of the NJL model, providing a semirigorous framework for studying the effect of the Cooper pairing on the physical properties of gluons.

The existence of the g2SC phase can be regarded as a physical and model independent result under the restriction of local charge neutrality condition, the order parameter for this phase is $\Delta < \delta\mu$. In Ref. [120], we calculated the gluon self-energy in the g2SC phase. It is found that, in this phase, the symmetry broken gauge bosons have imaginary Meissner screening masses, which is induced by the dominant paramagnetic contribution to the gluon self-energy. In condensed matter, this phenomenon is called the paramagnetic Meissner effect (PME) [138], and has been observed in some high temperature superconductors and small superconductors.

Unavoidably, the imaginary Meissner screening mass indicates a chromomagnetic instability of the g2SC phase. There are many proposals on resolving the chromomagnetic instability [139–143]: One is through a gluon condensate to stabilize the system, which may not change the structure of the g2SC phase. It is also possible that the instability drives a new stable ground state, which may have a rotational symmetry breaking like in

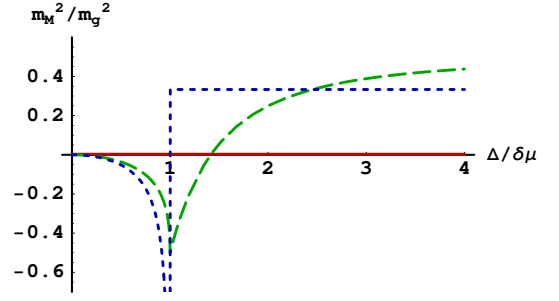


FIG. 18: Squared values of the gluon Debye (upper panel) and Meissner (lower panel) screening masses, divided by $m_g^2 = 4\alpha_s \bar{\mu}^2 / 3\pi$, as functions of the dimensionless parameter $\Delta / \delta\mu$. The red solid line denotes the results for the gluons with $A = 1, 2, 3$, the green long-dashed line denotes the results for the gluons with $A = 4, 5, 6, 7$, and the blue short-dashed line denotes the results for the gluon with $A = 8$. The figure is taken from Ref. [120].

Refs. [144, 145], or even have an inhomogeneous phase structure, like a crystal [99–101] or a vortex [146] structure.

D. Sarma instability and Higgs instability

In order to understand the chromomagnetic instability in the gapless phases, we extend the gauged NJL model beyond mean-field approximation [142]. The superconducting state is characterized by the order parameter $\Delta(x)$, which is a complex scalar field and has the form of $\Delta(x) = |\Delta(x)|e^{i\varphi(x)}$, with $|\Delta|$ the amplitude and φ the phase of the gap order parameter. For a homogeneous condensate, $\Delta(x)$ is a spatial constant. The fluctuations of the phase give rise to the pseudo Nambu-Goldstone boson(s), while that of the amplitude to the Higgs field, following the terminology of the electroweak theory. Stimulated by the role of the phase fluctuation in the unconventional superconducting phase [147] in condensed matter, we formulate the 2SC phase in the nonlinear realization framework [148] in order to naturally take into account the contribution from the phase fluctuation or pseudo Nambu-Goldstone current(s).

In the 2SC phase, the color symmetry $G = SU(3)_c$ breaks to $H = SU(2)_c$. The generators of the residual $SU(2)_c$ symmetry H are $\{S^a = T^a\}$ with $a = 1, 2, 3$ and the broken generators $\{X^b = T^{b+3}\}$ with $b = 1, \dots, 5$. (More precisely, the last broken generator is a combination of T_8 and the generator $\mathbf{1}$ of the global $U(1)$ symmetry of baryon number conservation, $B \equiv (\mathbf{1} + \sqrt{3}T_8)/3$ of generators of the global $U(1)_B$ and local $SU(3)_c$ symmetry.)

The coset space G/H is parameterized by the group

elements

$$\mathcal{V}(x) \equiv \exp \left[i \left(\sum_{a=4}^8 \varphi_a(x) T_a \right) \right], \quad (53)$$

here operator \mathcal{V} is unitary, and $\mathcal{V}^{-1} = \mathcal{V}^\dagger$ and $\varphi_a (a = 4, \dots, 7)$ and φ_8 are five Nambu-Goldstone diquarks, and we have not consider the topologically nontrivial case and therefore $\mathcal{V}(x)$ can be expanded uniformly according to the powers of φ 's. In fact, $\mathcal{V}(x)$ is always topologically trivial for a configuration of φ 's that has a finite energy because of the trivial homotopy group $\pi_2(SU(3)/SU(2))$.

Introducing a new quark field χ , which is connected with the original quark field q in Eq. (46) through a nonlinear transformation,

$$q = \mathcal{V} \chi, \quad \bar{q} = \bar{\chi} \mathcal{V}^\dagger, \quad (54)$$

and the charge-conjugate fields transform as

$$q_C = \mathcal{V}^* \chi_C, \quad \bar{q}_C = \bar{\chi}_C \mathcal{V}^T. \quad (55)$$

The advantage of transforming the quark fields is that this preserves the simple structure of the terms coupling the quark fields to the diquark sources,

$$\bar{q}_C \Delta^+ q \equiv \bar{\chi}_C \Phi^+ \chi, \quad \bar{q} \Delta^- q_C \equiv \bar{\chi} \Phi^- \chi_C. \quad (56)$$

In the Nambu-Gor'kov space of the new spinors

$$X \equiv \begin{pmatrix} \chi \\ \chi_C \end{pmatrix}, \quad \bar{X} \equiv (\bar{\chi}, \bar{\chi}_C), \quad (57)$$

the nonlinear realization of the original Lagrangian density Eq. (46) takes the form of

$$\mathcal{L}_{2SC}^{nl} \equiv -\frac{\Phi^+ \Phi^-}{4G_D} + \frac{1}{2} \bar{X} \mathcal{S}_{nl}^{-1} X, \quad (58)$$

with

$$\mathcal{S}_{nl}^{-1} \equiv \begin{pmatrix} [G_{0,nl}^+]^{-1} & \Phi^- \\ \Phi^+ & [G_{0,nl}^-]^{-1} \end{pmatrix}. \quad (59)$$

Here the explicit form of the free propagator for the new quark field is

$$[G_{0,nl}^+]^{-1} = i \not{D} + \hat{\mu} \gamma_0 + \gamma_\mu V^\mu, \quad (60)$$

and

$$[G_{0,nl}^-]^{-1} = i \not{D}^T - \hat{\mu} \gamma_0 + \gamma_\mu V_C^\mu. \quad (61)$$

Comparing with the free propagator in the original Lagrangian density, the free propagator in the non-linear realization framework naturally takes into account the contribution from the Nambu-Goldstone currents or phase fluctuations, i.e.,

$$\begin{aligned} V^\mu &\equiv \mathcal{V}^\dagger (i \partial^\mu) \mathcal{V}, \\ V_C^\mu &\equiv \mathcal{V}^T (i \partial^\mu) \mathcal{V}^*, \end{aligned} \quad (62)$$

which is the $N_c N_f \times N_c N_f$ -dimensional Maurer-Cartan one-form introduced in Ref. [148]. The linear order of the Nambu-Goldstone currents V^μ and V_C^μ has the explicit form of

$$V^\mu \simeq - \sum_{a=4}^8 (\partial^\mu \varphi_a) T_a, \quad (63)$$

$$V_C^\mu \simeq \sum_{a=4}^8 (\partial^\mu \varphi_a) (T_a)^T. \quad (64)$$

The advantage of the non-linear realization framework Eq. (58) is that it can naturally take into account the contribution from the phase fluctuations or Nambu-Goldstone currents. The task left is to find the correct ground state by exploring the stability against the fluctuations of the magnitude and the phases of the order parameters. The free energy $\Omega(V_\mu, \Phi, \mu, \mu_8, \mu_e)$ can be evaluated directly and it takes the form of

$$\begin{aligned} \Omega_{nl}(V_\mu, \Phi, \mu, \mu_8, \mu_e) &= -\frac{1}{2} T \sum_n \int \frac{d^3 \vec{p}}{(2\pi)^3} \text{Tr} \ln([S_{nl}(P)]^{-1}) \\ &\quad + \frac{\Phi^2}{4G_D}. \end{aligned} \quad (65)$$

In the 2SC phase, the color symmetry $SU(3)_c$ is spontaneously broken to $SU(2)_c$ and diquark field obtains a nonzero expectation value. Without loss of generality, one can always assume that diquark condenses in the anti-blue direction, i.e., only red and green quarks participate the Cooper pairing, while blue quarks remains as free particles. The ground state of the 2SC phase is characterized by $\langle \Delta^3 \rangle \equiv \Delta$, and $\langle \Delta^1 \rangle = 0$, $\langle \Delta^2 \rangle = 0$.

Considering the fluctuation of the order parameter, the diquark condensate can be parameterized as

$$\begin{aligned} \begin{pmatrix} \Delta^1(x) \\ \Delta^2(x) \\ \Delta^3(x) \end{pmatrix} &= \exp \left[i \left(\sum_{a=4}^8 \varphi_a(x) T_a \right) \right] \begin{pmatrix} 0 \\ 0 \\ \Delta + H(x) \end{pmatrix} \\ &\equiv \mathcal{V}(x) \Phi^\rho(x), \end{aligned} \quad (66)$$

where $\Phi^\rho(x) = (0, 0, \Delta + H(x))$ is the diquark field in the nonlinear realization framework, φ_a, φ_8 are Nambu-Goldstone bosons, and H is the Higgs field.

Expanding the diquark field Φ^ρ around the ground state: $\Phi^\rho = (0, 0, \Delta)$, the free-energy of the system takes the following expression as

$$\Omega_{nl} = \Omega_M + \Omega_{NG} + \Omega_H. \quad (67)$$

There are three contributions to the free-energy, the mean-field approximation free-energy part Ω_M has the form of

$$\Omega_M = -\frac{T}{2} \sum_n \int \frac{d^3 \vec{p}}{(2\pi)^3} \text{Tr} \ln([S_M(P)]^{-1}) + \frac{\Delta^2}{4G_D}, \quad (68)$$

the free-energy from the Higgs field Ω_H has the form of

$$\Omega_H = \frac{T}{2} \sum_{k_0} \int \frac{d^3 \vec{k}}{(2\pi)^3} H^*(K) \Pi_H(K) H(K) \quad (69)$$

with

$$\begin{aligned} \Pi_H(K) = & \frac{1}{2G_D} - \frac{T}{2} \sum_{p_0} \int \frac{d^3 \vec{p}}{(2\pi)^3} \text{Tr} \left[\mathcal{S}_M(P+K) \right. \\ & \left(\begin{array}{cc} 0 & i\tau_2 \epsilon^3 \gamma_5 \\ -i\tau_2 \epsilon^3 \gamma_5 & 0 \end{array} \right) \\ & \left. \mathcal{S}_M(P) \left(\begin{array}{cc} 0 & i\tau_2 \epsilon^3 \gamma_5 \\ -i\tau_2 \epsilon^3 \gamma_5 & 0 \end{array} \right) \right], \quad (70) \end{aligned}$$

and the free-energy from the Nambu-Goldstone currents Ω_{NG} has the form of

$$\begin{aligned} \Omega_{NG} = & -\frac{T^2}{4} \sum_{k_0} \sum_{p_0} \int \frac{d^3 \vec{k}}{(2\pi)^3} \frac{d^3 \vec{p}}{(2\pi)^3} \\ & \text{Tr} \left[\mathcal{S}_M(P+K) \left(\begin{array}{cc} \omega^\mu(-K) \gamma_\mu & 0 \\ 0 & \omega_C^\mu(-K) \gamma_\mu \end{array} \right) \right. \\ & \left. \mathcal{S}_M(P) \left(\begin{array}{cc} \omega^\mu(K) \gamma_\mu & 0 \\ 0 & \omega_C^\mu(K) \gamma_\mu \end{array} \right) \right], \quad (71) \end{aligned}$$

with

$$\omega^\mu(K) = g A_a^\mu(K) T_a - V^\mu(K), \quad (72)$$

$$\omega_C^\mu(K) = -g A_a^\mu(K) T_a^T + V_C^\mu(K). \quad (73)$$

where the inverse propagator \mathcal{S}_M^{-1} takes the form of

$$\begin{aligned} [\mathcal{S}_M(P)]^{-1} = & \left(\begin{array}{cc} [G_0^+(P)]^{-1} & i\tau_2 \epsilon^3 \gamma_5 \Delta \\ -i\tau_2 \epsilon^3 \gamma_5 \Delta & [G_0^-(P)]^{-1} \end{array} \right) \\ = & \gamma^0(p_0 + \rho_3 \hat{\mu}) - \vec{\gamma} \cdot \vec{p} + \Delta \rho_2 \tau_2 \epsilon^3 \gamma_5. \quad (74) \end{aligned}$$

The quasi-quark propagator at mean-field approximation has the form of

$$\mathcal{S}_M = \left(\begin{array}{cc} G^+ & \Xi^- \\ \Xi^+ & G^- \end{array} \right). \quad (75)$$

and its explicit expression of the Nambu-Gorkov components of \mathcal{S}_M has been derived in Ref. [120].

The Matsubara self-energy functions $\Pi_H(K)$ of the Higgs field and that of the Goldstone fields (obtained after the sum over p_0 and integral over \vec{p} in Eq. (71)) can be continued to real frequency following the standard procedure. Because of the gapless excitations, the values of these functions at zero frequency and zero momentum depends the order of the limit. In this work, we shall restrict our attention to static fluctuations only which amounts to replace $H(K)$, $\vec{A}(K)$ and $\varphi(K)$ of Eqs. (69) and (71) by $\sqrt{T}H(\vec{k})\delta_{k_0,0}$, $\sqrt{T}\vec{A}(\vec{k})\delta_{k_0,0}$ and $\sqrt{T}\varphi(\vec{k})\delta_{k_0,0}$. Thus the long wavelength limit of the self-energy functions discussed below corresponds to the limit $\lim_{\vec{k} \rightarrow 0} \lim_{k_0 \rightarrow 0}$.

Sarma instability

In the mean-field approximation, the free-energy for u, d quarks in β -equilibrium takes the form [118]:

$$\Omega_M = \frac{\Delta^2}{4G_D} - \sum_A \int \frac{d^3 p}{(2\pi)^3} \left[E_A + 2T \ln \left(1 + e^{-E_A/T} \right) \right]. \quad (76)$$

which is the same as Eq.(48) by neglecting the contribution of free electrons and taking zero quark mass in the color superconducting phase.

At zero temperature, the mean-field free-energy has the expression of

$$\begin{aligned} \Omega_M = & \frac{\Delta^2}{4G_D} - \frac{\Lambda^4}{2\pi^2} - \frac{\mu_{ub}^4}{12\pi^2} - \frac{\mu_{db}^4}{12\pi^2} \\ & - 2 \int_0^\Lambda \frac{p^2 dp}{\pi^2} \left(\sqrt{(p+\bar{\mu})^2 + \Delta^2} + \sqrt{(p-\bar{\mu})^2 + \Delta^2} \right) \\ & - 2\theta(\delta\mu - \Delta) \int_{\mu^-}^{\mu^+} \frac{p^2 dp}{\pi^2} \left(\delta\mu - \sqrt{(p-\bar{\mu})^2 + \Delta^2} \right). \quad (77) \end{aligned}$$

As we already knew that, with the increase of mismatch, the ground state will be in the gapless 2SC phase when $\Delta < \delta\mu$, the thermodynamical potential of which is given by

$$\Omega_M \simeq \Omega_M^{(0)} + \frac{2\bar{\mu}^2}{\pi^2} \left(\ln \frac{\delta\mu + \sqrt{\delta\mu^2 - \Delta^2}}{\Delta_0} - \delta\mu \sqrt{\delta\mu^2 - \Delta^2} + \delta\mu^2 \right) \quad (78)$$

where $\Omega_M^{(0)}$ is the normal phase thermodynamic potential. Δ_0 the solution to the gap equation in the absence of mismatch, $\delta\mu = 0$. The solution to the gap equation reads

$$\Delta = \sqrt{\Delta_0(2\delta\mu - \Delta_0)}. \quad (79)$$

The gapless phase is in principle a metastable Sarma state [132], i.e., the free-energy is a local maximum with respect to the gap parameter Δ . We have

$$\left(\frac{\partial^2 \Omega_M}{\partial \Delta^2} \right)_{\bar{\mu}, \delta\mu} = \frac{4\bar{\mu}^2}{\pi^2} \left(1 - \frac{\delta\mu}{\sqrt{\delta\mu^2 - \Delta^2}} \right). \quad (80)$$

The weak coupling approximation is employed in deriving Eqs. (78) and (80) from Eq. (77), which assumes that Δ_0 , Δ and $\delta\mu$ are much smaller than μ and $\Lambda - \mu$. The same approximation will be applied throughout the paper.

Nambu-Goldstone currents generation and the LOFF state

The quadratic action of the Goldstone modes in the long wavelength limit can be written down with the aid

of the Meissner masses evaluated in Ref.[120]. We find that

$$\Omega_{NG} = \frac{1}{2} \int d^3\vec{r} \sum_{a=1}^8 m_a^2 (\vec{A}^a - \frac{1}{g} \vec{\nabla} \varphi^a) (\vec{A}^a - \frac{1}{g} \vec{\nabla} \varphi^a) + \text{higher orders}. \quad (81)$$

where $m_1 = m_2 = m_3 = 0$,

$$m_4^2 = m_5^2 = m_6^2 = m_7^2 = \frac{g^2 \bar{\mu}^2}{3\pi^2} \left[\frac{\Delta^2 - 2\delta\mu^2}{2\Delta^2} + \theta(\delta\mu - \Delta) \frac{\delta\mu \sqrt{\delta\mu^2 - \Delta^2}}{\Delta^2} \right] \quad (82)$$

and

$$m_8^2 = \frac{g^2 \bar{\mu}^2}{9\pi^2} \left[1 - \frac{\delta\mu \theta(\delta\mu - \Delta)}{\sqrt{\delta\mu^2 - \Delta^2}} \right]. \quad (83)$$

It was found that at zero temperature, with the increase of mismatch, for five gluons with $a = 4, 5, 6, 7, 8$ corresponding to broken generator of $SU(3)_c$, their Meissner screening mass squares become negative [120]. This indicates the development of the condensation of

$$\sum_{a=4}^8 \langle \vec{A}^a - \frac{1}{g} \vec{\nabla} \varphi^a \rangle \neq 0. \quad (84)$$

It can be interpreted as the spontaneous generation of Nambu-Goldstone currents $\sum_{a=4}^8 \langle \vec{\nabla} \varphi^a \rangle \neq 0$ [139], or gluon condensation $\sum_{a=4}^8 \langle \vec{A}^a \rangle \neq 0$ [140]. It can also be interpreted as a colored-LOFF state [141] with the plane-wave order parameter

$$\Delta(x) = \Delta e^{i \sum_{a=4}^8 \vec{\nabla} \varphi^a \cdot \vec{x}}. \quad (85)$$

Higgs instability

We discussed the two known instabilities induced by mismatch, i.e., the Sarma instability and chromomagnetic instability, respectively. It is found that there is another instability, which is related to the Higgs field, and we call this instability "Higgs instability".

The free-energy from the Higgs field can be evaluated and takes the form of

$$\Omega_H = \frac{T}{2} \sum_{k_0} \int \frac{d^3\vec{k}}{(2\pi)^3} H^*(\vec{k}) \Pi_H(k) H(\vec{k}). \quad (86)$$

Evaluating the one-loop quark-quark bubble $\Pi_H(k)$, we obtain that

$$\Pi_H(k) = \frac{2\bar{\mu}^2}{\pi} I(k|\delta\mu) + \frac{\bar{\mu}^2}{2\pi\Delta^2} k^2 J(k|\delta\mu), \quad (87)$$

where the functions $I(k|\delta\mu)$ and $J(k|\delta\mu)$ are given by

$$I(k|\delta\mu) = \Delta^2 T \sum_n \frac{1}{\sqrt{(\omega_n + i\delta\mu)^2 + \Delta^2}} \int_{-1}^1 dx \frac{1}{(\omega_n + i\delta\mu)^2 + \Delta^2 + \frac{1}{4}k^2 x^2}, \quad (88)$$

$$J(k|\delta\mu) = \Delta^2 T \sum_n \frac{1}{\sqrt{(\omega_n + i\delta\mu)^2 + \Delta^2}} \int_{-1}^1 dx \frac{x^2}{(\omega_n + i\delta\mu)^2 + \Delta^2 + \frac{1}{4}k^2 x^2}. \quad (89)$$

with $\text{Re}\sqrt{(\omega_n + i\delta\mu)^2 + \Delta^2} > 0$. Here, the summation over n is the frequency summation at finite temperature field theory, with $\omega_n = (2n+1)\pi T$. At $T=0$, the free energy of the Higgs field has the form of

$$\Pi_H(k) = A_H + B_H k^2 \quad (90)$$

with

$$A_H = \left(\frac{\partial^2 \Omega_M}{\partial \Delta^2} \right)_{\delta\mu} = \frac{4\bar{\mu}^2}{\pi^2} \left(1 - \frac{\delta\mu}{\sqrt{(\delta\mu)^2 - \Delta^2}} \right), \quad (91)$$

$$B_H = \frac{2\bar{\mu}^2}{9\pi^2 \Delta^2} \left[1 - \frac{(\delta\mu)^3}{((\delta\mu)^2 - \Delta^2)^{\frac{3}{2}}} \right]. \quad (92)$$

It follows from Eqs. (91) and (92) that the Higgs field becomes unstable in the gapless phase when $\delta\mu > \Delta$, A_H in the gapless phase is shown in Fig. 19 by the red dash-dotted line. The Higgs instability was also considered in Ref. [143], where it was called as "amplitude instability". It has to be pointed out that we got different expressions for the coefficients of the gradient term. For $k \gg \Delta$, we have

$$\Pi_H(k) \simeq \frac{\bar{\mu}^2}{2\pi^2} \left(2 \ln \frac{k}{\Delta} - 2 - \ln \frac{\delta\mu - \sqrt{\delta\mu^2 - \Delta^2}}{\delta\mu + \sqrt{\delta\mu^2 - \Delta^2}} \right). \quad (93)$$

Therefore the Higgs instability disappears for sufficiently large momentum. The form factor $\Pi_H(k)$ for arbitrary momentum is plotted using red dashed line in Fig. 20 for a typical value of the mismatch parameter $\Delta/\delta\mu = 1/2$. We notice that the Higgs instability becomes stronger for nonzero momentum.

Charge neutrality condition

Unless a competing mechanism that results in a positive contribution to the inhomogeneous blocks of the stability matrix. The Higgs instability will prevent gapless superfluidity/ superconductivity from being implemented in nature. In the system of imbalanced neutral atoms, such a mechanism is not likely to exist and this contributes to the reason why the BP state has never been observed there. For the quark matter being considered, however, the positive Coulomb energy induced by the Higgs field of electrically charged diquark pairs has to be examined.

The second order derivative of the Hemholtz free energy for g2SC reads:

$$\left(\frac{\partial^2 \mathcal{F}}{\partial \Delta^2} \right)_{n_e} = \left(\frac{\partial^2 \Omega}{\partial \Delta^2} \right)_{\mu_e} + \frac{\left(\frac{\partial n_e}{\partial \Delta} \right)_{\mu_e}^2}{\left(\frac{\partial n_e}{\partial \mu_e} \right)_{\Delta}} \quad (94)$$

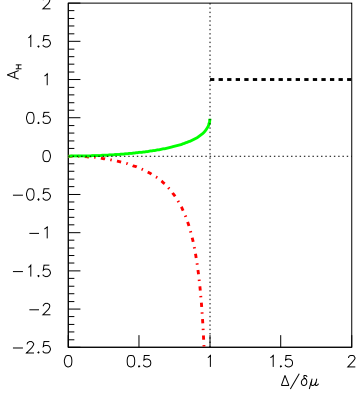


FIG. 19: Squared values of the gluon Debye (upper panel) and Meissner (lower panel) screening masses, divided by $m_g^2 = 4\alpha_s \bar{\mu}^2 / 3\pi$, as functions of the dimensionless parameter $\Delta/\delta\mu$. The red solid line denotes the results for the gluons with $A = 1, 2, 3$, the green long-dashed line denotes the results for the gluons with $A = 4, 5, 6, 7$, and the blue short-dashed line denotes the results for the gluon with $A = 8$. This figure is taken from Ref.[142].

and the stability implemented by the charge neutrality implies that

$$\left(\frac{\partial^2 \mathcal{F}}{\partial \Delta^2}\right)_{n_e} > 0. \quad (95)$$

While the global charge neutrality is maintained, an inhomogeneous ϕ will induce local charge distribution. The corresponding Coulomb energy

$$E_{\text{coul.}} = \frac{1}{2} \sum_{\vec{k} \neq 0} \frac{\delta \rho(\vec{k})^* \delta \rho(\vec{k})}{k^2 + m_D^2(k)}, \quad (96)$$

should be considered where $\delta \rho(\vec{k})$ is the Fourier component of the ϕ -induced charge density and m_D is the Coulomb polarization function (Debye mass at $\vec{k} = 0$). We have

$$m_D^2(k) = -\frac{e^2 T}{2} \sum_P \text{tr} \gamma_0 Q \mathcal{S}(P + K) \gamma_0 Q \mathcal{S}(P) \quad (97)$$

and

$$\delta \rho(\vec{k}) = \kappa(k) H(\vec{k}), \quad (98)$$

where

$$\kappa(k) = \frac{ieT}{2} \sum_P \text{tr} \gamma_0 Q \mathcal{S}(P + K) \gamma_5 \epsilon^3 \rho_2 \mathcal{S}(K) \quad (99)$$

with $K = (0, \vec{k})$ and Q the electric charge operator. We have

$$Q = \rho_3(a + b\tau_3) \quad (100)$$

with $a = 1/6$ and $b = 1/2$ for the quark matter consisting of u and d flavors.

The modified Higgs self-energy has the form of

$$\begin{aligned} \tilde{\Pi}_H(k) &\equiv \left(\frac{\partial^2 \mathcal{F}}{\partial H^*(\vec{k}) \partial H(\vec{k})} \right)_{n_e} \\ &= \left(\frac{\partial^2 \Omega}{\partial H^*(\vec{k}) \partial H(\vec{k})} \right)_{\mu_e} + \frac{\kappa^*(k) \kappa(k)}{k^2 + m_D^2(k)} \\ &= \Pi_H(k) + \frac{\kappa^*(k) \kappa(k)}{k^2 + m_D^2(k)}. \end{aligned} \quad (101)$$

The stability of the system with respect to the Higgs field requires that $\tilde{\Pi}_H(k) > 0$ for all k .

The form factor $\kappa(q)$ and the momentum dependent Debye mass square can be calculated explicitly at weak coupling, i.e. $\delta\mu \ll \bar{\mu}$ and $k \ll \bar{\mu}$. We find that

$$\kappa(k) = \frac{2e^2 \bar{\mu}^2 b}{\pi} K(k|\delta\mu) \quad (102)$$

with

$$\begin{aligned} K(k|\delta\mu) &= i\Delta T \sum_n \frac{\omega_n + i\delta\mu}{\sqrt{(\omega_n + i\delta\mu)^2 + \Delta^2}} \\ &\int_{-1}^1 dx \frac{1}{(\omega_n + i\delta\mu)^2 + \Delta^2 + \frac{1}{4}k^2 x^2} \end{aligned} \quad (103)$$

and

$$m_D^2(k) = \frac{6(a^2 + b^2)e^2 \bar{\mu}^2}{\pi^2} - \frac{2b^2 e^2 \bar{\mu}^2}{\pi} I(k|\delta\mu) \quad (104)$$

with the first term the Debye mass of the normal phase and $I(q|\delta\mu)$ the function defined in the section III.

Sarma instability at zero momentum limit can be removed by Coulomb energy:

Notice that

$$\lim_{k \rightarrow 0} \lim_{V \rightarrow \infty} \left(\frac{\partial^2 \Omega}{\partial H^*(\vec{k}) \partial H(\vec{k})} \right)_{\mu_Q} = \left(\frac{\partial^2 \Omega}{\partial \Delta^2} \right)_{\mu_Q}, \quad (105)$$

$$m_D^2(0) = e^2 \left(\frac{\partial n_e}{\partial \mu_e} \right)_{\Delta, \mu_B} \quad (106)$$

and

$$\kappa(0) = e \left(\frac{\partial n_e}{\partial \Delta} \right)_{\mu_e, \mu_B}. \quad (107)$$

We have

$$\lim_{k \rightarrow 0} \left(\frac{\partial^2 \mathcal{F}}{\partial H^*(\vec{k}) \partial H(\vec{k})} \right)_{\mu_e} = \left(\frac{\partial^2 \mathcal{F}}{\partial \Delta^2} \right)_{\mu_e}, \quad (108)$$

and the charge neutrality stabilize also the inhomogeneous Higgs field with the momentum much smaller

than the inverse coherence length and the inverse Debye length.

In the static long-wave length limit, we have

$$m_D^2(0) = \frac{2e^2 b^2 \bar{\mu}^2}{\pi^2} \left(1 + \frac{2\delta\mu}{\sqrt{\delta\mu^2 - \Delta^2}} \right) \quad (109)$$

and

$$\kappa(0) = \frac{4eb\bar{\mu}^2}{\pi^2} \frac{\Delta}{\sqrt{\delta\mu^2 - \Delta^2}}. \quad (110)$$

It follows from Eqs. (80), (101), (109) and (110) that the Higgs self-energy including Coulomb energy correction

$$\begin{aligned} \tilde{A}_H &\equiv \tilde{\Pi}_H(0) = \left(\frac{\partial^2 \mathcal{F}}{\partial \Delta^2} \right)_{\mu, n_Q} \\ &= \frac{4(b^2 - 3a^2)\bar{\mu}^2(\delta\mu - \sqrt{\delta\mu^2 - \Delta^2})}{\pi^2[3a^2\sqrt{\delta\mu^2 - \Delta^2} + b^2(2\delta\mu + \sqrt{\delta\mu^2 - \Delta^2})]}. \end{aligned} \quad (111)$$

is always positive for the whole range of g2SC state. It means that the Sarma instability in the gapless phase can be cured by Coulomb energy. This is shown in Fig. 19, where the red dash-dotted line indicates the A_H and the green solid line indicates \tilde{A}_H .

Higgs instability at nonzero momentum cannot be removed by Coulomb energy:

While the Sarma instability in g2SC phase can be cured by Coulomb energy under the constraint of charge neutrality condition, it is *not sufficient* for the system to be stable, even if the chromomagnetic instabilities are removed, say by gluon condensation. One has to explore the Higgs instability by calculating the self-energy function $\tilde{\Pi}(k)$ in the whole momentum space, which amounts to value the three basic functions $I(k|\delta\mu)$, $J(k|\delta\mu)$ and $K(k|\delta\mu)$ defined in (88), (89) and (103).

Fig. 20 shows the Higgs self-energy $\Pi_H(k)$ (the red dashed line) the Coulomb corrected Higgs self-energy $\tilde{\Pi}_H(k)$ (the black solid line) and the Coulomb energy E_{coul} (the green dash-dotted line) as functions of scaled-momentum k/Δ , in the case of $\delta\mu = 2\Delta$ and $(e^2\bar{\mu}^2)/(4\pi\Delta^2) = 1$.

Eventhough the Higgs instability can be removed by the Coulomb energy for small momenta, it returns for intermediate momenta. This phenomenon persists for a wide range of gap magnitude, $0 < \Delta < 0.866\delta\mu$ and for all strength of the Coulomb interaction, measured by the dimensionless ration $\eta \equiv \frac{\alpha_e\bar{\mu}^2}{\Delta^2}$. Within the narrow range $0.866\delta\mu < \Delta < \delta\mu$, the Higgs instability could be removed if the Coulomb interaction were sufficiently strong. For $\eta = 1$, We found that $\tilde{\Pi}_H(k) > 0$ for all k if $0.998\delta\mu < \Delta < \delta\mu$. In terms of the values of the parameters of NJL model, we have $\alpha_e\bar{\mu}^2 < \delta\mu$. Therefore the electric Coulomb energy cannot cure the Higgs instability for a realistic two flavor quark matter.

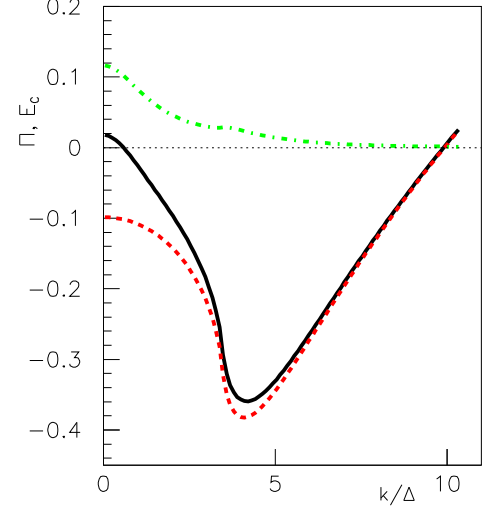


FIG. 20: The function $\Pi_H(k)$ (red dashed line), $\tilde{\Pi}_H(k)$ (black solid line) and the Coulomb energy (green dash-dotted line) as functions of scaled-momentum k/Δ , in the case of $\delta\mu = 2\Delta$ and $(e^2\bar{\mu}^2)/(4\pi\Delta^2) = 1$. This figure is taken from Ref.[142].

Negative $\Pi_H(k)$ indicates the Higgs mode is unstable and will decay [149]. It is noticed that $\Pi_H(k)$ reaches its minimum at a momentum, i.e., $k \simeq 4\Delta$, which indicates that a stable state may develop around this minimum, we characterize this momentum as k_{min} . The inverse k_{min}^{-1} is the typical wavelength for the unstable mode [150]. If mixed phase can be formed, the typical size l of the 2SC bubbles should be as great as k_{min}^{-1} , i.e., $l \simeq k_{min}^{-1}$ [150], which turns out to be comparable to the coherence length of 2SC in accordance with Eq. (79). (In the case of homogeneous superconducting phase, $k_{min} = 0$, and $l \rightarrow \infty$.) Considering that the coherence length ξ of a superconductor is proportional to the inverse of the gap magnitude, i.e., $\xi \simeq \Delta^{-1}$, therefore, a rather large ratio of k_{min}/Δ means a rather small ratio of l/ξ . When $l/\xi < 1$, a phase separation state is more favorable.

The reader has to keep in mind that our result of the Higgs instability only indicates some kind of inhomogeneous states whose typical length scale is comparable to the coherence length of 2SC. Further insight on the structure of the inhomogeneity cannot be gained without exploring the higher order terms of the nonlinear realization (66). A more direct approach to obtain the favorite structure of the ground state is to compare the free energy of various candidate states, which include the mixed phase, the single-plane wave FF state, striped LO state and multi-plane wave states. The Coulomb energy and the gradient energy have to be estimated reliably. We leave this analysis as a future project.

In the system of imbalanced neutral atoms, the Higgs

instability persists and induces spatial non-uniform phase separation state. This explains why imbalanced cold atom experiments did not observe LOFF state rather showed strong evidence of phase separation. For the 2-flavor quark matter being considered, the electric Coulomb interaction is not strong enough to compete with the Higgs instability.

IV. CONCLUSION

I have introduced several topics of QCD phase structure at high temperature and high density: the properties of strongly interacting quark gluon plasma, searching for the critical end point and the gapless color superconductor.

I give a brief introduction on the discovery of sQGP. It has been believed for more than 30 years that the QGP created at heavy-ion collisions should be weakly interacting gas system. However, a very small shear viscosity over entropy density ratio η/s is required to fit the RHIC data of elliptic flow v_2 . It is in contrary to the large value of η/s given by perturbative QCD calculation. This is a strong evidence that the deconfined matter created at RHIC is strongly interacted. The AdS/CFT duality gives a lower bound $\eta/s = 1/4\pi$. Therefore, it is conjectured that the sQGP created at RHIC might be the most perfect fluid observed in nature. However, a perfect fluid should have both vanishing shear and bulk viscosities. The property of the bulk viscosity of sQGP need to be studied before one draws the final conclusion.

Recent studies show that the bulk viscosity over entropy density ratio ζ/s rises up near phase transitions. The result from QCD effective models show that ζ/s be-

haves differently for different orders of phase transitions: for 1st-order phase transition, it rises sharply and show a divergent behavior, for the 2nd-order phase transition, it shows an upward cusp at T_c , for the case of crossover, the cusp becomes smooth. It is discussed that the sharp rising bulk viscosity will lead to the breakdown of hydrodynamics and affect the hadronization. Therefore the critical end point might be located through the observables which are sensitive to the ratio of bulk viscosity over entropy density.

The status of gapless color superconductor is reported. The chromomagnetic instability, the Sarma instability and Higgs instability are clarified. In the gapless color superconducting phase, both the phase part and magnitude part of the order parameter will develop instabilities: The phase part develops into the chromomagnetic instability, which induces the plane-wave state; The magnitude part develops the Sarma instability and Higgs instability, the Sarma instability can be competed with charge neutrality condition, while the Higgs instability cannot be cured by Coulomb interaction, and induces the inhomogeneous state.

V. ACKNOWLEDGEMENTS

I thank the collaboration with J.W.Chen, B.C.Li, H.Mao, D.L.Yang for the sQGP part, and I.Giannakis, D.Hou, H.C.Ren and I. Shovkovy for the gapless color superconductor part. The work is supported by CAS program "Outstanding young scientists abroad brought-in", CAS key project KJCX3-SYW-N2, NSFC10735040, NSFC10875134, and the K.C.Wong Education Foundation, Hong Kong.

-
- [1] D.J. Gross and F. Wilczek, Phys. Rev. Lett. 30 (1973) 1343; H.D. Politzer, Phys. Rev. Lett. 30 (1973) 1346.
 - [2] E. Klempt, hep-ph/0404270.
 - [3] T.D. Lee and G.C. Wick, Phys. Rev. D **9**, 2291 (1974).
 - [4] J.C. Collins and M.J. Perry, Phys. Rev. Lett. **34**, 1353 (1975).
 - [5] G. Baym and S.A. Chin, Phys. Lett. B **62**, 241 (1976).
 - [6] E.V. Shuryak, Phys. Lett. B **78**, 150 (1978).
 - [7] F. Karsch and E. Laermann, Phys. Rev. D **50**, 6954 (1994); F. Karsch, Nucl. Phys. A **698**, 199 (2002).
 - [8] E.V. Shuryak and I. Zahed, Phys. Rev. C **70**, 021901 (2004); E. Shuryak, Prog. Part. Nucl. Phys. **53**, 273 (2004); E.V. Shuryak and I. Zahed, Phys. Rev. D **70**, 054507 (2004); E.V. Shuryak, Nucl. Phys. A **750**, 64 (2005).
 - [9] D.H. Rischke, Prog. Part. Nucl. Phys. **52**, 197 (2004).
 - [10] M. Gyulassy and L. McLerran, Nucl. Phys. A **750**, 30 (2005).
 - [11] P. Jacobs and X.N. Wang, Prog. Part. Nucl. Phys. **54**, 443 (2005).
 - [12] U.W. Heinz, hep-ph/0407360.
 - [13] H.R. Jaqaman, A.Z. Mekjian, and L. Zamick, Phys. Rev. C **29**, 2067(1984); R.K. Su, F.M. Lin Phys. Rev. C **39**, 2438(1989).
 - [14] U.W. Heinz, P. R. Subramanian, H. Stocker and W. Greiner, J. Phys. G **12**, 1237 (1986).
 - [15] S.C. Frautschi, Asymptotic freedom and color superconductivity in dense quark matter, Proc.of the Workshop on Hadronic Matter at Extreme Energy Density, N. Cabibbo (Editor), Erice, Italy (1978).
 - [16] F. Barrois, Nucl. Phys. **B129** (1977),390.
 - [17] J. Bardeen, L.N. Cooper, J.R. Schrieffer *Phys. Rev.* 106:162 (1957); *Phys. Rev.* 108:1175 (1957).
 - [18] D. Bailin and A. Love, Phys. Rep. **107**, 325(1984).
 - [19] R. Rapp, T. Schäfer, E.V. Shuryak and M. Velkovsky, Phys.Rev.Lett.**81**,53(1998); M. Alford, K. Rajagopal and F. Wilczek, Phys.Lett.**B 422**,247(1998).
 - [20] K. Rajagopal and F. Wilczek, hep-ph/0011333; D.K. Hong, Acta Phys. Polon. B **32**, 1253 (2001); M. Alford, Ann. Rev. Nucl. Part. Sci. **51**, 131 (2001); G. Nardulli, Riv. Nuovo Cim. **25N3**, 1 (2002); T. Schäfer, hep-ph/0304281; M. Buballa, Phys. Rept. **407**, 205 (2005); H.C. Ren, hep-ph/0404074; M. Huang, Int. J. Mod. Phys. E **14**, 675 (2005); I. A. Shovkovy, Found.

- Phys. **35**, 1309 (2005); M. G. Alford, A. Schmitt, K. Rajagopal and T. Schafer, Rev. Mod. Phys. **80**, 1455 (2008); Q. Wang, arXiv:0912.2485 [nucl-th].
- [21] P. Arnold, G. D. Moore and L. G. Yaffe, JHEP **0305**, 051 (2003).
- [22] D. Teaney, J. Lauret and E. V. Shuryak, Phys. Rev. Lett. **86**, 4783 (2001), P. Huovinen, P. F. Kolb, U. W. Heinz, P. V. Ruuskanen and S. A. Voloshin, Phys. Lett. B **503**, 58 (2001), T. Hirano, U. W. Heinz, D. Kharzeev, R. Lacey and Y. Nara, Phys. Lett. B **636**, 299 (2006), P. Romatschke and U. Romatschke, Phys. Rev. Lett. **99**, 172301 (2007), H. Song and U. W. Heinz, Phys. Lett. B **658**, 279 (2008), H. Song and U. W. Heinz, Phys. Rev. C **77**, 064901 (2008).
- [23] D. Teaney, Phys. Rev. C **68**, 034913 (2003).
- [24] A. Nakamura and S. Sakai, Phys. Rev. Lett. **94**, 072305 (2005).
- [25] I. Arsene *et al.* [BRAHMS Collaboration], Nucl. Phys. A **757**, 1 (2005), K. Adcox *et al.* [PHENIX Collaboration], Nucl. Phys. A **757**, 184 (2005), B. B. Back *et al.*, Nucl. Phys. A **757**, 28 (2005), J. Adams *et al.* [STAR Collaboration], Nucl. Phys. A **757**, 102 (2005).
- [26] M. Gyulassy and L. McLerran, Nucl. Phys. A **750**, 30 (2005).
- [27] G. Policastro, D. T. Son and A. O. Starinets, Phys. Rev. Lett. **87**, 081601 (2001), P. Kovtun, D. T. Son and A. O. Starinets, Phys. Rev. Lett. **94**, 111601 (2005).
- [28] P. Arnold, C. Dogan and G. D. Moore, Phys. Rev. D **74**, 085021 (2006).
- [29] D. Kharzeev and K. Tuchin, JHEP **0809**, 093 (2008).
- [30] F. Karsch, D. Kharzeev and K. Tuchin, Phys. Lett. B **663**, 217 (2008).
- [31] H. B. Meyer, Phys. Rev. Lett. **100**, 162001 (2008).
- [32] K. Huebner, F. Karsch and C. Pica, Phys. Rev. D **78**, 094501 (2008).
- [33] K. Paech and S. Pratt, Phys. Rev. C **74**, 014901 (2006).
- [34] B. C. Li and M. Huang, Phys. Rev. D **78**, 117503 (2008); B. C. Li and M. Huang, Phys. Rev. D **80**, 034023 (2009).
- [35] J. W. Chen and J. Wang, Phys. Rev. C **79**, 044913 (2009).
- [36] C. Sasaki and K. Redlich, arXiv:0811.4708 [hep-ph].
- [37] G. Boyd, J. Engels, F. Karsch, E. Laermann, C. Legeland, M. Lutgemeier and B. Petersson, Nucl. Phys. B **469**, 419 (1996).
- [38] M. Cheng *et al.*, Phys. Rev. D **77**, 014511 (2008).
- [39] D. Fernandez-Fraile and A. G. Nicola, Phys. Rev. Lett. **102**, 121601 (2009); D. Fernandez-Fraile and A. G. Nicola, Eur. Phys. J. C **62**, 37 (2009).
- [40] G. Torrieri, B. Tomasik and I. Mishustin, Phys. Rev. C **77**, 034903 (2008); G. Torrieri and I. Mishustin, Phys. Rev. C **78**, 021901 (2008).
- [41] R. J. Fries, B. Muller and A. Schafer, Phys. Rev. C **78**, 034913 (2008).
- [42] T. Brasoveanu, D. Kharzeev and M. Martinez, Lect. Notes Phys. **785**, 341 (2010).
- [43] J. I. Kapusta, arXiv:0809.3746 [nucl-th].
- [44] Z. Fodor and S. D. Katz, J. High Energy Phys. **0203**, 014 (2002), P. de Forcrand and O. Philipsen, Nucl. Phys. Proc. Suppl. **129**, 521 (2004), F. Karsch, C. R. Allton, S. Ejiri, S. J. Hands, O. Kaczmarek, E. Laermann, and C. Schmidt, Nucl. Phys. Proc. Suppl. **129**, 614 (2004).
- [45] M. Asakawa and K. Yazaki, Nucl. Phys. A **504**, 668 (1989), A. Barducci, R. Casalbuoni, G. Pettini and R. Gatto, Phys. Rev. D **49**, 426 (1994), J. Berges and K. Rajagopal, Nucl. Phys. B **538**, 215 (1999), M. A. Hlasz, A. D. Jackson, R. E. Shrock, M. A. Stephanov and J. J. M. Verbaarschot, Phys. Rev. D **58**, 096007 (1998), P. Zhuang, M. Huang and Z. Yang, Phys. Rev. C **62**, 054901 (2000), O. Scavenius, A. Mocsy, I. N. Mishustin and D. H. Rischke, Phys. Rev. C **64**, 045202 (2001), N. G. Antoniou and A. S. Kapoyannis, Phys. Lett. B **563**, 165 (2003).
- [46] R.D. Pisarski and F. Wilczek, Phys. Rev. D **29**, 338 (1984).
- [47] Y. Hatta and T. Ikeda, Phys. Rev. D **67**, 014028 (2003); D. T. Son and M. A. Stephanov, Phys. Rev. D **70**, 056001 (2004); H. Fujii, Phys. Rev. D **67**, 094018 (2003); H. Fujii and M. Ohtani, Phys. Rev. D **70**, 014016 (2004); H. Fujii and M. Ohtani, Prog. Theor. Phys. Suppl. **153**, 157 (2004); K. Yagi, T. Hatsuda, Y. Miake, "Quark-Gluon Plasma, from big bang to little bang", Cambridge University Press.
- [48] M. A. Stephanov, K. Rajagopal, and E. V. Shuryak, Phys. Rev. Lett. **81**, 4816 (1998). M. A. Stephanov, K. Rajagopal, and E. V. Shuryak, Phys. Rev. D **60**, 114028 (1999).
- [49] R. A. Lacey *et al.*, Phys. Rev. Lett. **98**, 092301 (2007).
- [50] L. P. Csernai, J. I. Kapusta and L. D. McLerran, Phys. Rev. Lett. **97**, 152303 (2006).
- [51] S. S. Gubser, A. Nellore, S. S. Pufu and F. D. Rocha, Phys. Rev. Lett. **101**, 131601 (2008). S. S. Gubser, S. S. Pufu and F. D. Rocha, JHEP **0808**, 085 (2008).
- [52] J. W. Chen, M. Huang, Y. H. Li, E. Nakano and D. L. Yang, Phys. Lett. B **670**, 18 (2008).
- [53] H. Mao, J. Jin and M. Huang, arXiv:0906.1324 [hep-ph], to appear in J.Phys.G.
- [54] J.M. Cornwall, R. Jackiw, and E. Tomboulis, Phys. Rev. D **10**, 2428 (1974).
- [55] S. Jeon, Phys. Rev. D **52**, 3591 (1995); S. Jeon and L. Yaffe, Phys. Rev. D **53**, 5799 (1996).
- [56] B. J. Schaefer and M. Wagner, arXiv:0812.2855 [hep-ph].
- [57] K. Fukushima, Phys. Lett. B **591**, 277 (2004).
- [58] C. Ratti, M. A. Thaler and W. Weise, Phys. Rev. D **73**, 014019 (2006).
- [59] Z. Fodor and S. D. Katz, JHEP **0404**, 050 (2004).
- [60] W. j. Fu, Z. Zhang and Y. x. Liu, Phys. Rev. D **77**, 014006 (2008).
- [61] M. Ciminale, R. Gatto, N. D. Ippolito, G. Nardulli and M. Ruggieri, Phys. Rev. D **77**, 054023 (2008).
- [62] L. McLerran and R. D. Pisarski, Nucl. Phys. A **796**, 83 (2007).
- [63] G. D. Moore and O. Saremi, JHEP **0809**, 015 (2008).
- [64] A. Onuki, Phys. Rev. E **55**, 403 (1997).
- [65] L.N. Cooper, Phys. Rev. **104**, 1189 (1956).
- [66] W. Meissner and R. Ochsenfeld, Naturwiss. **21**, 787 (1933).
- [67] D.T. Son, Phys. Rev. D **59**, 094019 (1999).
- [68] T. Schafer and F. Wilczek, Phys. Rev. D **60**, 114033 (1999).
- [69] R.D. Pisarski and D.H. Rischke, Phys. Rev. D **61**, 074017 (2000).
- [70] R.D. Pisarski and D.H. Rischke, Phys. Rev. D **61**, 051501 (2000).
- [71] D.K. Hong, Phys. Lett. B **473**, 118 (2000).
- [72] D.K. Hong, V.A. Miransky, I.A. Shovkovy and L.C.R. Wijewardhana, Phys. Rev. D **61**, 056001 (2000); [Erratum-ibid. D **62**, 059903 (2000)].

- [73] W.E. Brown, J.T. Liu and H.C. Ren, Phys. Rev. D **61**, 114012 (2000); W.E. Brown, J.T. Liu and H.C. Ren, Phys. Rev. D **62**, 054016 (2000); W.E. Brown, J.T. Liu and H.C. Ren, Phys. Rev. D **62**, 054013 (2000).
- [74] C. Manuel, Phys. Rev. D **62**, 114008 (2000).
- [75] R. Rapp, T. Schafer, E.V. Shuryak and M. Velkovsky, Annals Phys. **280**, 35 (2000).
- [76] J. Berges and K. Rajagopal, Nucl. Phys. B **538**, 215 (1999).
- [77] G.W. Carter and D. Diakonov, Phys. Rev. D **60**, 016004 (1999).
- [78] T.M. Schwarz, S.P. Klevansky and G. Papp, Phys. Rev. C **60**, 055205 (1999).
- [79] R. Nebauer and J. Aichelin, Phys. Rev. C **65**, 045204 (2002).
- [80] M. Buballa, J. Hosek and M. Oertel, Phys. Rev. D **65**, 014018 (2002); M. Buballa and M. Oertel, Nucl. Phys. A **703**, 770 (2002).
- [81] D. Ebert, K.G. Klimenko and H. Toki, Phys. Rev. D **64**, 014038 (2001); D. Ebert, V.V. Khudiyakov, V.C. Zhukovsky and K.G. Klimenko, Phys. Rev. D **65**, 054024 (2002).
- [82] M. Huang, P.F. Zhuang and W.Q. Chao, Phys. Rev. D **65**, 076012 (2002).
- [83] T. Schafer and F. Wilczek, Phys. Lett. B **450**, 325 (1999).
- [84] N.J. Evans, S.D.H. Hsu and M. Schwetz, Nucl. Phys. B **551**, 275 (1999); N.J. Evans, S.D.H. Hsu and M. Schwetz, Phys. Lett. B **449**, 281 (1999); S.D.H. Hsu and M. Schwetz, Nucl. Phys. B **572**, 211 (2000).
- [85] D.H. Rischke, Phys. Rev. D **62**, 034007 (2000); D.H. Rischke and I.A. Shovkovy, Phys. Rev. D **66**, 054019 (2002).
- [86] M.G. Alford, K. Rajagopal and F. Wilczek, Nucl. Phys. B **537**, 443 (1999).
- [87] T. Schafer, Nucl. Phys. B **575**, 269 (2000).
- [88] N.J. Evans, J. Hormuzdiar, S.D.H. Hsu and M. Schwetz, Nucl. Phys. B **581**, 391 (2000).
- [89] I.A. Shovkovy and L.C.R. Wijewardhana, Phys. Lett. B **470**, 189 (1999).
- [90] D.H. Rischke, Phys. Rev. D **62**, 054017 (2000).
- [91] R. Casalbuoni and R. Gatto, Phys. Lett. B **464**, 111 (1999).
- [92] D. T. Son and M. A. Stephanov, Phys. Rev. D **61**, 074012 (2000); [Erratum-ibid. Phys. Rev. D **62**, 059902 (2000)].
- [93] T. Schafer and F. Wilczek, Phys. Rev. Lett. **82**, 3956 (1999).
- [94] T. Schafer, Phys. Rev. D **62**, 094007 (2000).
- [95] M. Buballa, J. Hosek and M. Oertel, Phys. Rev. Lett. **90**, 182002 (2003).
- [96] A. Schmitt, Q. Wang and D.H. Rischke, Phys. Rev. D **66**, 114010 (2002).
- [97] A. Schmitt, Q. Wang and D.H. Rischke, Phys. Rev. Lett. **91**, 242301 (2003); A. Schmitt, Q. Wang and D.H. Rischke, Phys. Rev. D **69**, 094017 (2004).
- [98] A. Schmitt, nucl-th/0405076.
- [99] A.I. Larkin, YuN. Ovchinnikov, *Zh. Eksp. Teor. Fiz.* **47** (1964), 1136; translation: *Sov. Phys. JETP* **20** (1962), 762.
- [100] P. Fulde, R.A. Ferrell, Phys. Rev. **135**, A550 (1964).
- [101] M.G. Alford, J.A. Bowers and K. Rajagopal, Phys. Rev. D **63**, 074016 (2001).
- [102] J.A. Bowers, J. Kundu, K. Rajagopal and E. Shuster, Phys. Rev. D **64**, 014024 (2001).
- [103] A.K. Leibovich, K. Rajagopal and E. Shuster, Phys. Rev. D **64**, 094005 (2001).
- [104] J. Kundu and K. Rajagopal, Phys. Rev. D **65**, 094022 (2002).
- [105] J.A. Bowers and K. Rajagopal, Phys. Rev. D **66**, 065002 (2002).
- [106] J.A. Bowers, hep-ph/0305301.
- [107] I. Giannakis, J.T. Liu and H.C. Ren, Phys. Rev. D **66**, 031501 (2002).
- [108] R. Casalbuoni and G. Nardulli, Rev. Mod. Phys. **76**, 263 (2004); R. Casalbuoni, M. Ciminale, M. Mannarelli, G. Nardulli, M. Ruggieri and R. Gatto, Phys. Rev. D **70**, 054004 (2004); R. Casalbuoni, R. Gatto, M. Mannarelli, G. Nardulli and M. Ruggieri, Phys. Lett. B **600**, 48 (2004).
- [109] T. Schafer, Phys. Rev. Lett. **85**, 5531 (2000); P.F. Bedaque and T. Schafer, Nucl. Phys. A **697**, 802 (2002).
- [110] D.B. Kaplan and S. Reddy, Phys. Rev. D **65**, 054042 (2002).
- [111] T. Schafer, D.T. Son, M.A. Stephanov, D. Toublan and J.J.M. Verbaarschot, Phys. Lett. B **522**, 67 (2001).
- [112] V.A. Miransky and I.A. Shovkovy, Phys. Rev. Lett. **88**, 111601 (2002).
- [113] M. Rho, A. Wirzba and I. Zahed, Phys. Lett. B **473**, 126 (2000);
- [114] D.K. Hong, T. Lee and D.P. Min, Phys. Lett. B **477**, 137 (2000).
- [115] C. Manuel and M.H.G. Tytgat, Phys. Lett. B **479**, 190 (2000).
- [116] T. Schafer, Phys. Rev. D **65**, 074006 (2002).
- [117] A. Kryjevski, D.B. Kaplan and T. Schafer, Phys. Rev. D **71**, 034004 (2005).
- [118] I. Shovkovy and M. Huang, Phys. Lett. B **564**, 205 (2003).
- [119] M. Huang and I. Shovkovy, Nucl. Phys. A **729**, 835 (2003).
- [120] M. Huang and I.A. Shovkovy, Phys. Rev. D **70**, 051501 (2004); M. Huang and I.A. Shovkovy, Phys. Rev. D **70**, 094030 (2004).
- [121] M. Alford, C. Kouvaris and K. Rajagopal, Phys. Rev. Lett. **92**, 222001 (2004); M. Alford, C. Kouvaris and K. Rajagopal, Phys. Rev. D **71**, 054009 (2005).
- [122] K. Iida, T. Matsuura, M. Tachibana and T. Hatsuda, Phys. Rev. Lett. **93**, 132001 (2004).
- [123] S.B. Ruster, I.A. Shovkovy and D.H. Rischke, Nucl. Phys. A **743**, 127 (2004).
- [124] K. Fukushima, C. Kouvaris and K. Rajagopal, Phys. Rev. D **71**, 034002 (2005).
- [125] A. Kryjevski and T. Schaefer, Phys. Lett. B **606**, 52 (2005).
- [126] M. Alford and K. Rajagopal, JHEP **0206**, 031 (2002).
- [127] A.W. Steiner, S. Reddy and M. Prakash, Phys. Rev. D **66**, 094007 (2002).
- [128] M. Huang, P.F. Zhuang and W.Q. Chao, Phys. Rev. D **67**, 065015 (2003).
- [129] S.B. Ruster, Diploma thesis, J. W. Goethe-University, 2003. S.B. Ruster and D.H. Rischke, Phys. Rev. D **69**, 045011 (2004).
- [130] A. Mishra and H. Mishra, Phys. Rev. D **69**, 014014 (2004).
- [131] K. Rajagopal and F. Wilczek, Phys. Rev. Lett. **86**, 3492 (2001).
- [132] G. Sarma, J. Phys. Chem. Solids **24**, 1029(1963).

- [133] M.G. Alford, J. Berges and K. Rajagopal, Phys. Rev. Lett. **84**, 598 (2000).
- [134] W.V. Liu and F. Wilczek, Phys. Rev. Lett. **90**, 047002 (2003); W.V. Liu, F. Wilczek and P. Zoller, Phys. Rev. A **70**, 033603 (2004); M.M. Forbes, E. Gubankova, W.V. Liu and F. Wilczek, Phys. Rev. Lett. **94**, 017001 (2005).
- [135] E. Gubankova, W.V. Liu and F. Wilczek, Phys. Rev. Lett. **91**, 032001 (2003).
- [136] E. Gubankova, E. G. Mishchenko and F. Wilczek, Phys. Rev. Lett. **94**, 110402 (2005).
- [137] S.B. Nam, Phys. Rev. **156**, 470 (1967).
- [138] A.K. Geim, S.V. Dubonos, J.G.S. Lok, M. Henini, and J.C. Maan, Nature **396**, 144 (1998); M. Sigrist, T.M. Rice, Rev. Mod. Phys. **67**, 503 (1995); Mai Suan Li, Phys. Rept. **376**, 133(2003).
- [139] D. K. Hong, hep-ph/0506097; Mei Huang, Int. J. Mod. Phys. A **21**, 910 (2006); Mei Huang, Phys. Rev. D **73**, 045007 (2006); A. Kryjevski, Phys. Rev. D **77**, 014018 (2008); T. Schafer, Phys. Rev. Lett. **96**, 012305 (2006); A. Gerhold and T. Schafer, Phys. Rev. D **73**, 125022 (2006).
- [140] E. V. Gorbar, M. Hashimoto and V. A. Miransky, Phys. Lett. B **632**, 305 (2006); M. Hashimoto, Phys. Lett. B **642**, 93 (2006).
- [141] I. Giannakis and H. C. Ren, Phys. Lett. B **611**, 137 (2005); I. Giannakis and H. C. Ren, Nucl. Phys. B **723**, 255 (2005); I. Giannakis, D. f. Hou and H. C. Ren, Phys. Lett. B **631**, 16 (2005);
- [142] I. Giannakis, D. Hou, M. Huang and H. c. Ren, Phys. Rev. D **75**, 011501 (2007); I. Giannakis, D. Hou, M. Huang and H. c. Ren, Phys. Rev. D **75**, 014015 (2007).
- [143] K. Iida and K. Fukushima, Phys. Rev. D **74**, 074020 (2006).
- [144] H. Muther and A. Sedrakian, Phys. Rev. D **67**, 085024 (2003).
- [145] E. Nakano, T. Maruyama and T. Tatsumi, Phys. Rev. D **68**, 105001 (2003); T. Tatsumi, T. Maruyama and E. Nakano, hep-ph/0312351.
- [146] A.A. Abrikosov, Sov.Phys.JETP **5**, 1174(1957) [Zh. Eksp. Theo. Fiz. **32**, 1442 (1957)].
- [147] H. Kleinert, cond-mat/9503030; M.Franz, Z. Tesanovic, Phys.Rev.Lett.87, 257003(2001); M.Franz, Z. Tesanovic, O.Vafek, Phys.Rev.**B66**(2002), 054535; A. Melikyan, Z. Tesanovic, cond-mat/0408344.
- [148] R. Casalbuoni, Z. y. Duan and F. Sannino, Phys. Rev. D **62**, 094004 (2000); V. A. Miransky, I. A. Shovkovy and L. C. R. Wijewardhana, Phys. Rev. D **64**, 096002 (2001); D. H. Rischke and I. A. Shovkovy, Phys. Rev. D **66**, 054019 (2002).
- [149] S. R. Coleman and E. Weinberg, Phys. Rev. D **7**, 1888 (1973); S. R. Coleman, Phys. Rev. D **15**, 2929 (1977), [Erratum-ibid. D **16**, 1248 (1977)].
- [150] E. J. Weinberg and A. q. Wu, Phys. Rev. D **36**, 2474 (1987).